Polymer Based Voltammetric Sensors

Paolo Ugo

Department of Physical Chemistry, University of Venice, Santa Marta, Venice, Italy

CONTENTS

1. GENERAL INTRODUCTION

1.1. Historical Background

The first pioneering studies published at the beginning of the 1980s, carried out in Anson's, Bard's, Murray's and other laboratories [1–4], showed the possibility to build microstuctures on electrodes surfaces by simply depositing via dip-coating, microvolume evaporation or spin-coating a thin layer of a polymer film on the electrode surface. Depending on the functional groups linked to the polymer backbone, this procedure allowed to obtain electrodes able to sense redox ions which can interact with the coating. These first studies opened the way to extended research efforts which brought rapidly to the development of a large arsenal of polymer modified electrodes whose surface properties were tailored for specific analytical purposes [5–7]. All these studies and applications were based on the quite simple concept that a regular metal electrode can acquire special properties useful for analytical and sensing purposes by coating its surface with a suitable polymer film.

Few years later, Martin's group [8, 9], shortly followed by Uosaki and coworkers [10], proposed a new idea: use a preformed microporous membrane to build specially featured electrodes inside the membrane, so obtaining an integrated membrane-electrode(s) device. Such integrated nanostructured electrode systems were initially built using alumina microporous membranes [8–10] which were later substituted by track-etched polycarbonate nanoporous membranes to prepare what was called nanoelectrode ensembles (NEE) [11, 12]. Commercially available track-etched polymeric ultrafiltration membranes (developed for sophisticated biological separations) were used to this aim. These membranes contain monodispersed pores of very small diameter which were used as templates to build ensembles and arrays of micro- and nanoelectrodes. Both in film-coated electrodes and in membrane templated NEEs, the chemical and physical properties of the polymer layer play a key role in determining the success and the specific application of the polymer-based electrode device. Note that both procedures can be used in a combined way so that even polymer coated NEEs can be obtained [12].

Most recent advancements in the field of membrane-based electrode systems came on one side from improvements of the techniques used for controlling the molecular structure of ultrathin polymer layers (Langmuir-Blodgett, self-assembled monolayers, layer-by-layer techniques [13, 14]) and on the other from continuous progress and development in the template synthesis of metal nanostructures such as nanowires, nanotubes or nanocapsules [15]. Nanostructured electrode interfaces can be ranked, indeed, as successful examples of the buttom-up approach, which, in nanoscience terminology is the capability to obtain functional materials whose properties are the result of the careful and controlled assembly of different molecular bricks which fulfill specialized functions in a device (sensor).

Interestingly, the capability of suitably modifying electrode surfaces and using templating microporous membranes for preparing micro- and nanoelectrodes arrays are presently founding a large impulse, also in concomitance with their exploitation as electrochemical sensors in advanced biomedical devices [16]. It is worth pointing out that the majority of the studies on polymer coated electrodes performed in the 1980s employed a variety of Ru, Ir, Os, Fe complexes as electroactive reversible probes used for understanding the fundamentals of charge transfer at electrode/polymer interfaces. At that time, the electrochemistry of such metal complexes was considered of almost no interest as far as practical applications were concerned; nowadays, many of such molecules are widely used as redox mediators in a variety of biosensors, included some of the most advanced DNA-chips [16–18].

The present chapter will progress following the historical evolution of researches in the field; after a brief general overview to introduce electrochemical methods of analysis, it will deal with basic principles up to more recent developments in electrochemical sensing with polymer coated electrodes; then, it will discuss the use of micro- and nanoporous

polymer membranes for building nanoelectrodes ensembles, focusing on their application for advanced molecular recognition purposes.

1.2. Brief Introduction to Voltammetry

This paragraph will give some short basic notions on electrochemical methods of analysis, useful for understanding the functioning and better appreciating most recent advancements in voltammetric sensors, which constitutes the core of this chapter. Readers interested in a deeper insight on fundamentals and applications of electroanalytical techniques are addressed to specialized textbooks [19, 20].

The analytes detected by electrochemical methods are redox species, i.e., molecules or ions which can release (or acquire) electrons to (from) proper reactants (molecules or metal surfaces) characterized by oxidizing (or reducing) properties.

From a classification viewpoint, electrochemical methods of analysis are divided in equilibrium methods (potentiometry) and dynamic ones (polarography, amperometry, voltammetry, coulometry and others) [19, 20].

In the former, no current circulate through the electrochemical cell and the tendency of a certain redox reaction to occur is obtained by measuring the open circuit electrochemical potential (E(OC)) of the cell; it is linked to the concentration of redox species in the electrolyte solution by the Nernst equation.

In dynamic (or transient) electrochemical techniques, a net current (or charge) is obtained as the result of an external excitation (generally a voltage waveform) applied to the electrochemical cell; since such a current signal obeys Faraday's law, it is named Faradaic current. Experimental conditions are chosen so that the system operates under concentration polarization conditions and the Faradaic current (at proper applied potentials) is a function of the concentration in the electrolyte solution of the redox species (analyte) being reduced or oxidized at the electrode.

In voltammery, the quantity being measured is the intensity of the electrical current which circulates through the circuit composed by the so-called working electrode (which is the "sensing" electrode), the electrolyte solution and the counter electrode (a large area electrode, with polarity opposite to the working electrode).The excitation waveform is given as an electrical potential applied (and changed in a known manner) to the working electrode with respect to a third electrode, which acts as an unpolarized reference electrode (generally a second species electrode, e.g., an Ag/AgCl electrode).

In linear sweep and in cyclic voltammetry (CV), the potential (E_{appl}) applied to the working electrode changes linearly with time (t) according to Eq. (1):

$$E_{appl} = E_i + vt \tag{1}$$

where E_i is the initial potential which is lower than the Nernst potential ($E°$) of the redox couple (i.e., $|E_i| < |E°|$); v is the scan rate (in V/s or mV/s).

Really, in CV the potential is scanned forward and backward (once or many times, depending on the measurement mode used) from E_i (where no Faradic current is observed,

since $|E_i < E°|$) to move (with a certain scan rate) toward a vertex potential (E_v chosen so that $|E_v| > |E°|$) where a net current corresponding to the Faradic reduction (or oxidation) of the analyte is observed. In the backward scan (from E_v to E_i), the opposite electrode process occurs, which corresponds roughly to the return to the initial redox state of the product generated; if the forward process is a reduction, the process expected in the backward scan is the re-oxidation of reduction products.

Transport of the analyte from the bulk solution to the electrode/solution interface can take place only by diffusion, since convection and migration are inhibited by keeping the solution quiet, by avoiding thermal gradients (eventually by a thermostat) and by making negligible the effect of the applied electric field by adding an excess supporting electrolyte (electrochemically inert).

With planar electrodes of dimensions larger than the thickness of the diffusion layer (see below), i.e., in the millimeter size range, diffusion follows the so-called semi-infinite planar diffusion model. The CV obtained under this diffusion regime is characterized by two associated voltammetric peaks, one recorded during the forward scan and one in the backward scan. The two peaks are located at potential values symmetric with respect to a characteristic potential value named half-wave potential ($E_{1/2}$). For reversible redox couples $E_{1/2} = (Ep_f + Ep_b)/2$, where Ep_f and Ep_b are the potential of the forward and backward peak, respectively; $E_{1/2}$ is strictly related to $E°$ [19, 20]. If the analyte is an oxidized species, then the forward peak corresponds to the direct process:

$$Ox + ne \rightarrow Red \tag{2}$$

and the backward peak to the reverse process (from electro-generated Red back again to Ox).

Note that in voltammetry, an electrochemical process is considered reversible when the charge transfer process between the analyte and the electrode is faster than mass transport (diffusion). Therefore, under diffusion control and when $|E_{appl}| \gg |E°|$, a concentration gradient is generated between the electrode surface (where the concentration of analyte is zero since all redox molecules which come or are on the electrode surface are reduced) and the bulk of the solution (where the concentration is the initial analyte concentration). The region where a concentration gradient exists is called diffusion layer. Under these conditions, the Faradaic current relevant to reaction (2) depends on the rate with which the analyte diffuses from the bulk solution to the electrode surface, this being inversely proportional to the thickness of the diffusion layer. This points out that voltammetric responses are time dependent, since the thickness of the diffusion layer, δ, depends on time according to Eq. (3)

$$\delta = (D \times t)^{1/2} \tag{3}$$

where D is the diffusion coefficient of the analyte (in cm²/s) and t is the time scale of the experiment. Note that, in voltammetry t depends on the scan rate according to:

$$t = RT/Fv \tag{4}$$

Scan rates normally used in voltammetry are between 0.020–1.000 V s^{-1} and diffusion coefficients for solution species are of the order of 10^{-5}–10^{-6} cm^2/s, so that it is easily estimated that the thicknesses of diffusion layers are in the micrometer scale. This will be relevant when using electrodes with some peculiar dimensions (electrode diameter or thickness of electrode coatings) in such or even smaller dimension range.

The Faradaic current signal (S) is not the only current being measured by voltammetric electrodes; an electrode dipped in an electrolyte solution behaves, in fact, also as a capacitor and a certain amount of current (charging current) is consumed to build up the so-called electrical double layer [19, 20]. The double layer charging current increases with the electrode area and with the scan rate. Moreover, also other small currents, named residual currents and related to the electroactivity of trace concentrations of redox impurities, can interfere with the recording of the Faradaic current of the analyte. In voltammetry, double layer charging currents and residual currents constitutes the main component of the noise (N). The voltammetric S/N ratio can be improved by using the so-called pulsed voltammetric techniques, such as differential pulse voltammetry (DPV) or Osteryoung's square wave voltammetry (SWV) [19, 20]. These electroanalytical techniques use excitation waveforms which are the combination of linear (or staircase) potential ramps with superimposed sequences of short potential pulses (10–50 mV for 10–50 ms). Proper sampling and combination of current values measured at fixed time lag with respect to the pulses application allow significant improvements in S/N ratios and consequent lowering of detection limit (DL) values. In fact, while with classical cyclic voltammetry (where no noise reduction is applied) DL are typically in the 10^{-4} M range, with pulsed techniques DLs go down to the 10^{-6}–10^{-7} M range. More recently, newly advanced pulsed techniques such as, for instance, multiple square wave voltammetry (MSWV) [21, 22] and double-differential MSWV [23, 24], allowed even further lowering of voltammetric DLs.

The already low DLs achievable by using these pulsed techniques can be improved by introducing a preconcentration step before the voltammetric detection. The preconcentration of the analyte is performed directly at the transducer (electrode) surface via Faradaic (for anodic, ASV, or cathodic, CSV, stripping voltammetry) [25] and/or non Faradaic (adsorption, ion-exchange, complexation, etc.) processes; this allows one to reach DLs as low as 10^{-11}–10^{-12} M.

1.3. Advantages and Limits of Classical Electroanalytical Devices

Dynamic electrochemical methods of analysis have some advantageous peculiarities which make them good candidates for sensing purposes. First of all they take advantage of the immediate transduction of chemical information into an electrical signal, the Faradaic current, which is produced directly at the electrode-solution interface and which depends linearly on the analyte concentration (and not logarithmically as in potentiometry). Transient techniques are very sensitive and they allow one to work rather easily at very low detection limits. In addition, they can give information on the redox state and complexation of the analyte in the sample [27]. They can be used in turbid or colored samples and do not suffer for interference from ambient light. However, in some cases, dissolved oxygen (which is electroactive) can constitute a problem and should be eliminated; indeed some experimental tricks which allow one to shorten or even avoid the necessity to eliminate dissolved oxygen, have been presented in the recent literature [28, 29]. All these characteristics make, in principle, electrochemical methods and sensors attractive for determining redox analytes at trace (micromolar) and ultratrace (submicromolar) concentration levels in complex samples such as those of interest, for instance, in environmental monitoring or for biomedical analyses.

However, up to recent time, some limits to the widespread use of dynamic electrochemical methods came from the fact that a great part of these methods were based on the use of mercury as electrode material. Mercury has some advantages in electroanalysis, and, really, the very first dynamic electroanalytical method, polarography for which Jaroslav Heyrowski won the Nobel Prize in 1959, was based on the use of the dropping mercury electrode. However, because of the high toxicity of mercury, nowadays there is increasing interest in developing methods which employ different electrode materials. Note that, in addition to toxicity related problems, the use of mercury electrodes suffers also from other limitations. Even the most recent mercury drop electrode systems are still rather expensive and cumbersome, they use relatively high amounts of mercury and are rather complicate for set up of unmanned automatic analyses. Recently, silver-mercury amalgam [30] and bismuth [31] have been proposed as alternatives for mercury. However, mercury as well as these alternative materials cannot be used at positive potential values because of their easy oxidation, so that all the world of oxidation processes is precluded to this kind of electrodes.

In order to widen the application field of electroanalytical methods it is important to develop novel electrode systems characterized by high sensitivity, good reproducibility, wide usable potential window, low cost and made of non-toxic materials. Moreover, they should be characterized by intrinsic molecular recognition properties so that they can give specific responses in complex real samples and can be used even for automatic continuous monitoring. Obviously this is not an easy task, also because interferences and artifacts are always a possible important source of mistake, however some significant steps in this direction have been moved recently, also thanks to the development of new nanostructured and polymer based electrode systems.

2. POLYMER FILMS ON ELECTRODES

2.1. Ion-Exchange Voltammetry with Polymer Coated Electrodes

The advantage of coating the metal surface of an electrode with a thin film of a functionalized polymer is found in the capability of exploiting the reactivity of the polymer functional groups to develop some specific interaction with the analyte [32]. A sketch of a polymer-coated electrode is shown in Fig. 1.
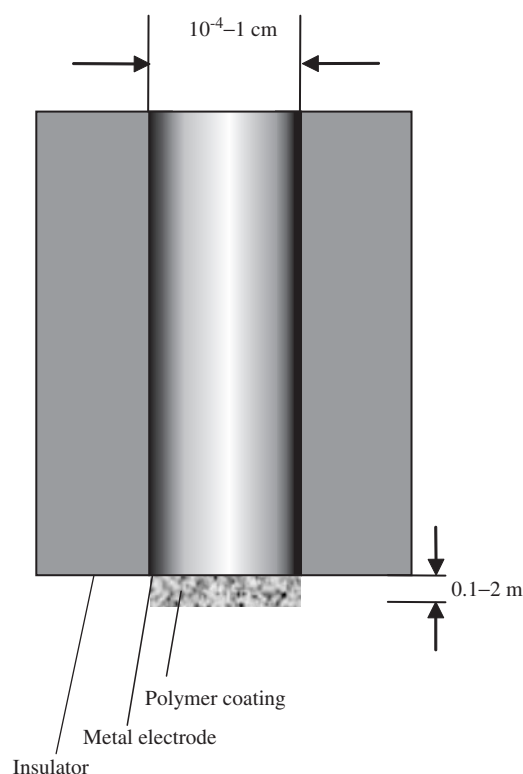
Figure 1. Schematic drawing of a polymer coated metal disk electrode.

Depending on the chemical nature of these functional groups, the reaction can be a complexation or a ion-exchange reaction. Both two kinds of interactions present some general similarities, at least as far as the way by which the analyte preconcentration process influences the voltammetric signal; however, the energetics and the nature of the reactions involved are significantly different. In both cases, the interaction of the analyte with the polymer causes on one side a local increase of the analyte concentration and, on the other hand, a decrease of its mobility (lowering of diffusion coefficients). Both for ion-exchange and complexation, the preconcentration effects are quantified by an equilibrium constant which can be an ion-exchange distribution coefficient [33] or the formation constant of a complex species [26], respectively. The preconcentration of the analyte at the electrode/coating interface causes an increase in voltammetric signals, which however is somehow contrasted by the lowering of diffusion coefficients caused by the interaction of the analyte with the polymer layer. Usually, higher is the preconcentration constant, lower is the mobility of the analyte in the coating. In voltammetric terms, optimizing the preconcentration means finding the best compromise between these two opposite effects.

As typical examples of polymer coated electrodes, the following part of this chapter will focus on electrodes modified with ion-exchangers coatings, that is a field that generated many practical examples of applications for chemical analysis and sensing [5, 6].

First examples of voltammertic measurements performed with electrodes coated with thin films of ion-exchangers were published in 1980 by Anson's and Bard's groups [1, 2]. The

term ion-exchange voltammetry (IEV) was introduced few years later in a paper by Martin's group [34]. This technique employs solid electrodes (usually glassy carbon, gold or platinum disk electrodes) coated by a thin layer (usually 0.1–2 μm thick) of an ion-exchange polymer which allows the quick preconcentration and simultaneous voltammetric detection of ion redox analytes [5]. The voltammetric signal recorded in these conditions depends on the concentration and apparent diffusion coefficient (D_{app}) of electroactive species incorporated by ion-exchange inside the polymeric layer. If an ion-exchanger characterized by proper selectivity is used, it is possible to determine trace and ultratrace levels of ionic electroactive analytes. Moreover, the presence of a polyionic coating on the electrode surface prevents adsorption or precipitation phenomena favored by the presence in the sample of organics and surfactants [35–38]. These is a situation commonly encountered for the case of analysis in complex matrices such as environmental or biological samples.

2.2. Principles of Ion-Exchange Voltammetry

For simplicity, principles of IEV are discussed here for the case of the preconcentration and electrochemical one-electron reduction of a cationic oxidized analyte, M^{n+}, at an electrode coated with a polyanionic film containing, for instance, sulphonic groups as ion-exchange sites. Analogue considerations can be obtained, with the proper easy corrections, for IEV of anionic oxidized species on a polycationic coated electrode and for reduced cationic or anionic analytes as well.

The preconcentration capability of the coating is ruled by the ion-exchange equilibrium between the electroactive counter-ion (analyte) and nonelectroactive counter-ions present in solution or already incorporated into the coating, according to the following reaction [33]:

$$M^{n+} + n(SO_3^- X^+) \leftrightarrow n(SO_3^-)M^{n+} + X^+ \qquad (5)$$
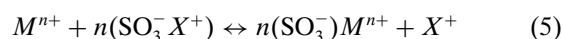
where: SO_3^- are the ion-exchange sites in the polymer, X^+ is an electrochemically inert counter-ion (for simplicity a cation of charge $z = 1$, as generally is the supporting electrolyte cation, e.g., Na^+), M^{n+} is the multiply charged electroactive analyte.

The extent of such equilibrium reaction is expressed quantitatively by the selectivity coefficient (K_X^M):

$$K_X^M = \{[M^{n+}]_p[X^+]_s^n\}/\{[M^{n+}]_s[X^+]_p^n\} \qquad (6)$$

where subscripts p and s indicate concentrations in the polymer and solution phases, respectively and square bracket indicates molar concentrations. With proper adaptations [5], ionic equivalent fractions can be used instead of molar concentartions. In some cases, a corrected selectivity coefficient is used, where activity coefficients of the solution species are used instead of concentrations. It is worth stressing that the selectivity coefficient is not strictly constant, but can depend on experimental conditions [33].

When the ion-exchanged analyte is a trace species, the changes in $[X^+]_s$ and $[X^+]_p$ can be negligible and the selectivity coefficient can be conveniently substituted by the distribution coefficient, k_D, given as:

$$k_{D(M^{n+})} = [M^{n+}]_p/[M^{n+}]_s \qquad (7)$$

It is obvious that the analyte will be preconcentrated by coatings characterized by $k_D > 1$.

When a reducing electrochemical potential is applied (i.e., $E_{appl} < E°$), M^{n+} is reduced at the polymer/electrode interface and a voltammetric peak is correspondingly recorded. If, as stated above, the reduction is a one-electron process (i.e., number of electrons exchanged, $n = 1$), reaction (8) holds [39, 40]:

$$n(SO_3^-)M^{n+} + e^- + X^+ \leftrightarrow (n-1)(SO_3^-)M^{(n-1)+} + SO_3^- X^+ \qquad (8)$$
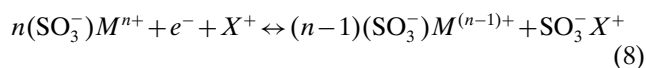
Under proper experimental conditions (three-electrodes electrochemical cell; mass transport controlled by seminfinite planar diffusion), the voltammetric reduction current is a function of the concentration of electroactive species incorporated into the coating. It is interesting to note that the open circuit electrochemical potential at the coated electrode ($E(OC)_{CE}$), obtained by applying the Nernst equation to reaction (8), is given by:

$$E(OC)_{CE} = E°' + (RT/F) \log\{[X^+]_s/[X^+]_p\} + (RT/F) \log\{[M^{n+}]_p/[M^{(n-1)+}]_p\} \qquad (9)$$

where $E°'$ is the formal potential of the incorporated redox couple at the ionic strength of the coating; ionic activities have been approximated by their concentrations. Equation (9) can be easily rearranged for cases where n or $z \neq 1$.

It was shown [39, 41, 42] that, when differences in diffusion coefficients of oxidized and reduced species are negligible, the half-wave potential obtained by IEV at the coated electrode, $(E_{1/2})_{IEV}$, exhibited by the redox couple within the coating is given by:

$$(E_{1/2})_{IEV} = E°' + (RT/F) \log\{[X^+]_s/[X^+]_p \qquad (10)$$

The partitioning of the oxidized and reduced species between the solution and the coating is ruled by relevant distribution coefficients; Eq. (7) for the oxidized analyte is complimented by Eq. (11) relevant to the reduced partner:

$$[M^{(n-1)+}]_p = k_D(M^{(n-1)+})[M^{(n-1)+}]_s \qquad (11)$$

By proper substitution one gets:

$$E(OC)_{CE} = E°' + (RT/F)\{ \log[X^+]_s/[X^+]_p) + \log(k_D(M^{n+})/k_D(M^{(n-1)+})) + \log([M^{n+}]_s/[M^{(n-1)+}]_s)\} \qquad (12)$$

This equation is important for cases where both redox partners M^{n+} and $M^{(n-1)+}$ are present in the sample. In particular, when the concentration of electroactive analytes M^{n+} and $M^{(n-1)+}$ is low, almost all the ion-exchange sites are saturated by X^+ so that changes in $[X^+]_p$ are negligible [43] and Eq. (10) can be rearranged as:

$$E(OC)_{CE} = K + (RT/nF) \log([M^{n+}]_s/[M^{(n-1)+}]_s) \qquad (13)$$

where:

$$K = E°' + (RT/nF) \log(k_D(M^{n+})/k_D(M^{(n-1)+})) + (RT/F) \log([X^+]_s/[X^+]_p) \qquad (14)$$

This means that open circuit potential values, $E(OC)_{CE}$, measured by potentiometry [43] at the polymer coated electrode, change linearly with $\log([M^{n+}]_s/[M^{(n-1)+}]_s)$ with a slope equal to $59/n$ mV (at $20°C$) and with an intercept given by Eq. (14). If all the other terms are independently known, $E(OC)_{CE}$ values allow one to calculate the concentration ratio in the sample solution between the redox species M^{n+} and $M^{(n-1)+}$. Equation (13) is rather similar to the usual Nenst equation for a redox indicator electrode [20] with the advantage that the coated electrode can preconcentrate the redox ions so, in principle, it can be used for trace analysis; moreover, the coating rejects interfering species of opposite ionic charge than the analyte.

These principles are the basis for performing redox state speciation of trace analytes of environmental interest, as for instance Fe^{2+} and Fe^{3+} cations [43], by using ionomer coated electrodes. By combining ion-exchange voltammetric and potentiometric data (with both data sets obtained at the same polymer coated electrode) it is possible to obtain quantitative information on speciation. Ion-exchange voltammetry is used for quantifying total concentrations and for obtaining relevant k_D values (see below), potentiometry at the coated electrode is employed for obtaining the concentration ratio between chemical species characterized by different redox states.

2.3. Current Responses at Polymer Coated Electrodes

Many research papers have been devoted to study the mechanisms which rules mass and charge transport phenomena in polymeric matrices (see Refs. [44–46] for reviews). Depending on the experimental conditions involved (mainly, type of polymer, redox properties and concentration of the ion-exchanged analvte), the overall transport process can be controlled by a variety of phenomena such as physical diffusion of redox species, electron hopping, segmental motion of polymer chains, polymer diffusion, counter-ion migration and ion pairing [44, 45]. Regardless the microscopic mechanism, such transport phenomena obeys Fick's law of diffusion and the rate of transport depends on an observable parameter characteristic for the analyte (and polymer layer) and named apparent diffusion coefficient, D_{app}.

As for voltammetric experiments performed at the electrode/solution interface, also at polymer coated electrodes peak currents are determined by the dimensions and time dependence of the diffusion layer which (for the polymer case) is the region of the electrode/polymer interface where an analyte concentration gradient is generated by the applied potential. Note that, at polymer coated electrodes, the rate limiting step which determines current responses

is diffusion through the electrode/polymer interface. It is therefore important to distinguish whether the measurements are carried out in a time scale, t, for which the thickness of the diffusion layer δ is smaller or larger than the thickness of the polymeric coating, Φ. This determines the existence of two different kinds of voltammetric responses, typical of polymer coated electrodes, which are [4]:

(a) a linear diffusion controlled behavior, when $\delta \gg \Phi$;
(b) a thin-layer like behavior, when $\delta \gg \Phi$.

The passage from situation (a) to situation (b) depends on relevant values of the coating thickness and voltammetric scan rate. Under conditions (a), there is a pool outside the diffusion layer which furnishes fresh analyte able to diffuse to the electrode in the time course of the scan; for case (b), the analyte incorporated in the coating is reduced (or oxidized) exhaustively during the voltammetric scan. As illustrated in Fig. 2, the characteristics of the voltammograms recorded under the two conditions are very different:

• under semi-infinite linear diffusion conditions. the voltammetric peak shows the classical diffusive tail due to the Cottrellian current decay observed at potential values cathodic enough with respect to the peak potential [see Fig. 2(a)]; the peak current depends on the square root of v, according to easy re-arrangement [5]
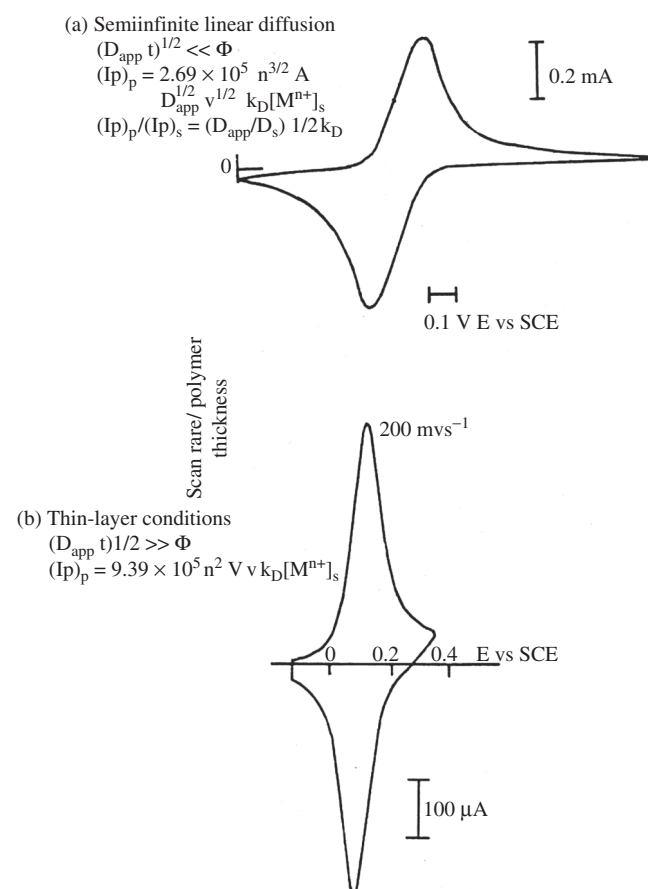
Figure 2. Typical mass and charge transfer regimes observed at polymer coated electrodes as a function of the scan rate and/or thickness of the polymer layer. See text for symbols in the equations.

of the classical Randles-Sevcik equation, where D_{app} substitutes D and $[M^{n+}]_p = k_D[M^{n+}]_s$ substitutes the bulk solution concentration;
• for a thin-layer-like behavior, the voltammetric peak shows a characteristic symmetric Gaussian shape [see Fig. 2(b)]; the peak current Ip depends linearly on the scan rate v, according to Eq. (15) [4]:

$$(Ip)_p = 9.39 \times 10^5 n^2 vV[M^{n+}]_p \qquad (15)$$

Signal given by Eq. 15, are independent on D_{app}, but depends on the film volume V. This means that the peak current in thin-layer-like conditions increases with the film volume and thickness. From a practical point of view, compatibly with an acceptable ohmic drop effect due to the increased film thickness and the necessity to keep operative thin-layer-like conditions, i.e., $(D_{app}t)^{1/2} > \Phi$, electrodes coated with thicker films are expected to give thin-layer-like responses characterized by higher sensitivity. As said before, the possibility of working in thin-layer-like or diffusion-controlled conditions can be assured by choosing a proper scan rate.

Measurements under thin-layer like conditions are useful also for measuring voltammetrically the amount of analyte incorporated in the polymer layer after equilibration with a certain concentration of analyte in the sample solution; this quantity is obtained, in fact, via coulometric integration of the voltammetric peak recorded in thin-layer-like conditions (low scan rate, generally 2–5 mV/s). The plots $[M^{n+}]_p$ vs. $[M^{n+}]_s$ at constant temperature give the ion-exchange distribution isotherms from which one can calculate relevant K_X^M or k_D values [see Eqs. (6) and (7)] [47, 48].

On the other hand, ion-exchange voltammetric signals recorded under semi-infinite planar diffusion conditions are strongly influenced by D_{app} values. The ratio between peak currents recorded in the same experimental conditions at unmodified, $(Ip)_s$, and at polymer coated electrodes, $(Ip)_p$, (of the same surface area A and with both electrodes operating under semi-infinite planar diffusion control) is given by Eq. (16):

$$(Ip)_p/(Ip)_s = (D_{app}/D_s)^{1/2}k_D \qquad (16)$$

This equation shows that the factor $(D_{app}/D_s)^{1/2}k_D$ plays the role of an amplification factor which quantifies the increase of voltammetric signals when polymer coated electrodes are used instead of bare ones. D_{app} values are typically in the 10^{-9}–10^{-12} cm^2/s range [44–46]; they are 2–3 orders of magnitude lower than D_s values (usually in the 10^{-9}–10^{-12} cm^2/s range [44–46]). Because of such a large difference in diffusion coefficient values, the ion-exchange preconcentration results effective in increasing voltammetric signals for those analytes who are characterized by ion-exchange distribution coefficient values $k_D > 100$–1000. In such cases, the increase in sensitivity can then be of several orders of magnitude.

Without entering into a detailed analysis of the dynamics of electron transport in ion-exchanger coatings, it is worth noting that the operativity of different microscopic charge transfer mechanisms can have consequences also for the analytical application of IEV, since it can cause the appearance of a dependence of D_{app} (and therefore of $(Ip)_p$)

on $[M^{n+}]_p$. Although such complications can be considered more exceptions than the rule, however the possibility that D_{app} changes with $[M^{n+}]_p$ cannot be neglected.

For instance, if electron hopping between the redox centers incorporated into the polymeric coating is the rate determining step [3, 49, 50], than D_{app} can increase with $[M^{n+}]_p$ [51, 52]. In According to the Dahms-Ruff electron hopping model [45, 53, 54], D_{app} is given as:

$$D_{app} = (1/6)k_{ex}d^2[M^{n+}]_p \qquad (17)$$

where k_{ex} = site to site electron exchange rate constant; d = distance of closest approach between two neighboring sites.

In other cases, the incorporation of a multiply charged analyte which can interact electrostatically with more than one polymeric chain can cause a sort of electrostatic crosslinking effect which reflects in a decrease of D_{app} with increasing $[M^{n+}]_p$ [55–60]. With electrodes modified with perflourosulfonate ionomers, the decrease of diffusion coefficients with increasing concentration was explained by a bottleneck effect caused by the narrow channels that interconnect ionic clusters in these polymers [55]. It was recently shown that changes in the microenvironment within the ionomeric coating can influence such a behavior [61].

2.4. Analytical Applications

The electrode coating most widely used in IEV of redox cations is probably Nafion® followed by the sulphonated polyesters such those belongings to the Eastman AQ series. For anionic analytes, poly(4-vinylpyridine) and Tosflex® IE-SA 48 (produced by Tosoh Co., Japan) are the most used polymeric coatings. Nafion®, Tosflex® and sulfonated polyesters (see Scheme 1) belong to the ionomer group that are ionic polymers characterized by a rather low content of ionic groups [62].

These ionic groups generally interact or associate to form ion-rich hydrophilic regions surrounded by hydrophobic domains [63], such a clustering being the basis of the high stability of ionomer films.
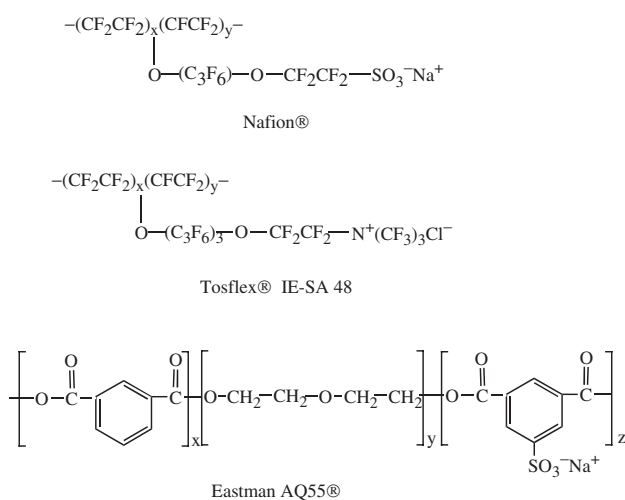
Scheme 1

The easiness of modification of the electrode surface and mechanical and chemical stability of ionomer coatings explain their successful use in IEV. The physical properties of Nafion® such as density, ion-exchange capacity etc. which are relevant to the successful preparation and analytical application of coated electrodes have been the subject of careful studies by Leddy's group [64–66].

Apart ionomers, also other ion-exchangers were applied for ion-exchange voltammetry such as, for instance, poly(4-vinylpyridine) [1], poly(2-vinylpyrazine) [41], poly(L-lysine) and derivatives [67]. However, because of the higher water solubility of these polyelectrolytes which contain a large number of ion-exchange sites, the preparation of stable coatings require a chemical crosslinking stabilization procedure (see Section 2.5.1), which make their use a little more complicated than that of ionomers.

Specific analytical applications of IEV at polymer coated electrodes have been reviewed recently [5, 6], (see Ref. [68] for IEV with inorganic ion-exchangers).The following Tables 1–3, list some typical analytical applications of electrodes modified with ionomers and related polymers; they show that a quite large number of sensing applications of IEV have been developed up to now. The majority of the methods listed are characterized by very low detection limits, in the 10^{-9}–10^{-11} M range, with relatively short ion-exchange preconcentration time (typically <20 min). In many cases, the use of ion-exchanger coated electrodes can reduce drastically the effects of interferences and allows one to perform trace speciation analysis [6], that is to identify and to measure the concentration of one or more individual chemical species of the same element.

Details on the methods listed can be found in the cited original papers.

2.5. Practical Considerations

2.5.1. Classical Methods of Coating Depositions

Different ways of film deposition can be used [4], the simplest and more popular procedure being casting a microvolume of polymer solution onto the electrode surface,

Table 1. Examples of ion-exchange voltammetry of inorganic cations at ionomer coated electrodes.

Analyte	Modifier	Ref.
Pb^{2+}	Nafion®	[69,70]
	Nafion®/1-(2-pyridylazo)-2-naphtol	[71]
Pb^{2+}, Cu^{2+}	Nafion®	[36,72]
Pb^{2+}, Cu^{2+}, Cd^{2+}	Nafion®	[35]
Zn^{2+}	Nafion®	[73]
Pb^{2+}, Cu^{2+},	Nafion®	[74]
Cd^{2+}, Zn^{2+}	Nafion®/poly(vinylsulphonic acid)	[37]
	Polyester sulphonate	[38]
Tl^+	Nafion®	[75]
Tl^+, Pb^{2+}	Nafion®	[76]
$Fe^{2+/3+}$	Nafion®	[4, 77, 78]
CH_3Hg^+	Nafion®	[23]
Eu^{3+}	Nafion®	[24,79]
Eu^{3+}, Yb^{3+}	Nafion®	[80,81]
UO_2^{2+}	Nafion®	[48]

Table 2. Examples of ion-exchange voltammetry of organic cations at ionomer coated electrodes.

Analyte	Modifier	Ref.
Viologen	Polyester sulphonate	[82, 83]
	Nafion®	[84]
	Nafion®/tetraethoxysilane	[85]
	Nafion®/clay	[86]
N-nitrosamines	Sulphopolyester (Eastek)	[87]
Parathion	Nafion®	[88]
Phenol	Nafion®	[89]
Dopa, Epinephrine,	Nafion®	[90, 91]
Norephinephrine	Polyester sulphonate	[92]
Dopamine, Serotonine	Nafion®	[93–95]
	Polyester sulphonate	[96]
Adenine	Nafion®	[97]
4-nitroso-N,N-diethylaniline	Nafion®	[98]
Promethiazine	Nafion®	[99]
Salbutamol, Fenoterol,	Nafion®	[100]
Metaproterenol		
Phenazine ethosulphate	Polyester sulphonate	[101]
Apomorphine	Nafion®	[102]
Tert-butylhydroquinone	Nafion®	[103]

then allowing the solvent to evaporate slowly. This procedure has been used successfully for modifying electrodes starting from alcohol-water solutions of the perfluorinated cation-exchanger Nafion® [2, 122] or Tosflex® [117, 123]. Film uniformity can be improved by resorting to the spin-coating procedure [124, 125]. However, particular care must be devoted to avoid partial removing of the polymer solution by centrifugal force while spinning the electrode, otherwise any information on the amount of deposited modifier will be lost. Droplet-evaporation and₁'or spin-coating have been

Table 3. Examples of ion-exchange voltammetry of anionic analytes at ionomer coated electrodes.

Analyte	Modifier	Ref.
Cr^{VI}	Protonated poly (4-vinylpyridine)	[104, 105]
I^-	Tosflex®	[106]
Br^-	Tosflex®	[42]
$HgCl_4^{2-}$	Tosflex®	[107, 108]
	Poly(3-pyrrol-1-ylmethylpyridinium)	[109, 110]
Bi^{III}	Tosflex®	[111]
	Poly (4-vinylpyridine)	[112]
$TeCl_6^{2-}$	Tosflex®/8-quinolonol	[113]
Zn^{II}	Tosflex®	[114]
Pb^{II}	Quaternized poly (4-vinylpyridine)	[115]
$CuCl_2^-$	Quaternized poly (4-vinylpyridine)	[116]
	Tosflex®	[117]
Se^{IV}	Tosflex®/3,3′-diaminebenzidine	[118]
Uric acid, catechol, ascorbic acid, acetaminophen	Protonated poly (4-vinylpyridine)	[119]
Ascorbic acid	Poly(3-pyrrol-1-ylmethylpyridinium)	[120]
O,O-Diethyldithiophosphoric acid	Tosflex®	[121]

used also for casting coatings of poly(estersulfonic acid) of the Eastman AQ series. However, in this case, stable films are obtained only after heating the deposited polymer at temperatures of about 60—80 °C [126] or by dissolving the ionomer in a water-acetone mixture of proper composition [83].

Nafion®, Tosflex® and Eastman AQ are characterized by high equivalent weights and by a low number of ion-exchange sites interposed between long organic chains. This makes the structure of the solvated coating a clusterlike structure in which hydrophobic and hydrophilic domains exist [63], the hydrophobic zones being responsible for adsorption and stabilization of such coatings on hydrophobic electrode materials such as glassy carbon and pyrolytic graphite.

The influence of some parameters such as composition of the polymer solution and drying temperature [127–130], humidity [131, 132] or other treatments such as RF-plasma treatment [133] on the structure, stability and ion-exchange behavior of recasted coatings has been studied.

Polymeric materials characterized by low equivalent weights, which behave as true polyelectrolytes and are characterized by higher water solubilities, have been used to recast polymer films on electrode surfaces by microvolume evaporation. However, with these materials a chemical crosslinking stabilization procedure is required. A typical example is given by poly(4-vinylpyridine), which gives more stable and reproducible coatings when the polymer backbone is crosslinked by reacting with alkyldihalides a fraction of the pyridinic nitrogen atoms [134, 135]. This procedure was used also for other polymers containing heterocyclic nitrogen, such as poly(2-vinylpyrazine) [41]. Note that poly(4-vinylpyridine) behaves as an anion-exchanger when the pyridinic nitrogen is in the pyridinium form, e.g., protonated by dipping the modified electrode in solution at pH < 5.2 [1], or quaternized by reaction with alkyl halides [136]. Crosslinking of polyelectrolytes can be obtained also by irradiation methods, as for the case of poly(dimethvldiallylammonium chloride) [137].

Another popular and effective way of preparing ion-exchange coatings is electropolymerization [4], this procedure being used for depositing films of electroactive polymers prepared by polymerization of electroactive monomeric precursors. They can be redox polymers (see e.g., [138]), conducting polymers [139] or functionalized conducting polymers [109, 120, 140–142]. However, in principle, performing ion-exchange voltammetry with electrodes coated with polymers which are electroactive themselves, can suffer some limitations since the electroactivity window relevant to the polymer can overlap with the detection window of some analytes. On the other hand, the signal relevant to the electroactive moiety of the polymer can be used to good advantage as an internal standard to evaluate signals quantitatively [143].

As above mentioned, electrochemical oxidation is used to electropolymerize anionic or cationic derivatives of pyrrole [140–142], so obtaining coatings in which the potential dependent ion-exchange properties typical of conducting polymers are enhanced and become independent on the applied potential. Moreover, functionalization of polypyrrole with fixed ion-exchange sites increases its ion-exchange

capacity about 4 times [141], compared with plain polypyrrole in its fully oxidized form. Electrochemical polymerization is used for the preparation of coatings which incorporate the electroactive mediators used in electrochemical biosensors. These approach has been introduced some years ago by Heller and coworkers [144,145] originating a class of electroactive polymeric materials tailored for the electrochemical "wiring" of redox enzymes and other biomacromolecules.

2.5.2. Molecular Engineering of Ionomer Deposition

Advances in the reliable use of polymer coated electrodes for analytical purposes depend on improvements in the control and reproducibility of the deposition of the polymer layer. This allows also the lowering of the film thickness and shortening of the response time. Moreover, molecular control of the coating structures allows the deliberate control of the hydrophobic/hydrophilic properties as well as clustering and surface exposures of the ion-exchange sites.

Hoyer et al. [146] presented recently an electrostatic spray deposition method which allows the preparation of very uniform thin films (ca. 0.3 μm), keeping unaltered the peculiar features of Nafion® as far as permselectivity and rejection of interferents are concerned.

New possibilities to built ordered structures of ionomer films on a smaller scale (nanometer) can come by the application of layer-by-layer deposition techniques [14]. The layer-by-layer strategy allows the construction of supramolecular sandwiches, assembled by exploiting electrostatic interactions. It is based on the alternate deposition of molecular layers of cationic and anionic (poly)ions arranged in sandwiched ordered structures thanks to favorable electrostatic interactions between the layers of opposite charge. Typical examples of application of the layer-by-layer strategy to the preparation of modified electrodes and sensors can be found in the recent biosensors literature [147–154]. For the specific case of ionomeric materials, an example was presented recently, where a thin film consisting of alternating layers of Nafion® and ferric ions was used [155] to develop new calcification-resistant implantable biosensors [155] or other nanolayered materials [156–158].

Other possibilities in the molecular engineering of ionomer films on electrodes surfaces were opened recently, by studying the preparation and characteristics of ionomer coatings prepared by using the Langmuir-Blodgett (LB) technique [13]. It is used to build up monolayers or multilayers of organic amphiphilic molecules in which the order and 2-D structure are controlled at the molecular level by controlling the compression extent in the LB trough of a monomolecular layer of the amphiphilic molecules, spread at the air/water interface. By this way, it is possible to obtain ultrathin films characterized by long range order, which can provide new insights on electron transfer processes at molecularly ordered interfaces. The 2-D ordered interfacial layer can be transferred on solid surfaces by controlled dipping through the interface. There are two ways of dipping the substrate: the classical Langmuir-Blodgett technique (vertical transfer) and the Langmuir-Schaefer (LS) technique (horizontal transfer). The LS technique is usually employed for the transfer of rigid films of materials such as polymers. The substrate touches the monolayer horizontally, than it is inclined and moved up. Although the LS technique showed to work well for Nafion® [159], it has the limitation to rely upon the manual ability and experience of the experimentalist. Very recently it was shown that successful transfer of Langmuir layers of ionomers can be achieved also by optimizing the conditions for the classical LB technique which is a vertical dipping-lift deposition technique for which the rate and extent of the movement of the substrate through the interfacial film is controlled automatically by a mechanical dipper driven by suitable software.

It was shown that if proper electrolyte is dissolved in an aqueous subphase, Nafion® forms an interfacial film at the air-water interface, which can be compressed in a typical Langmuir-Blodgett experiment, giving a stable film transferable on the surface of a variety of materials, including electrode surfaces [159, 160]. The thickness of the Nafion® film transferred can be as thin as few nanometers and scales with the number of layers deposited. The film keeps the performances typical of thicker Nafion® coatings as far as permselectivity and incorporation of multiply charged cations are concerned. However, because of the much smaller thickness of the coating, ion-exchange equilibration is faster.

Langmuir-Blodgett and Langmuir-Schaefer deposition procedures can be used also for other ionomers such as Tosflex® and Eastman AQ55® [161]. The condensation degree of the interfacial film depends on the nature of the electrolyte dissolved in the subphase, as reflected also by significant lowering of D_{app} values relevant to ion-exchanged redox probes [160].

As far as stability and condensation degree are concerned, perfluorinated polymers such as Nafion® and Tosflex® showed better properties than the polyester sulphonated Eastman AQ55®, the former being useable for many days of ion-exchange voltammetric measurements. Electrodes modified with LB films of ionomers showed ion-exchange-preconcentration capabilities useful for ion-exchange voltammetric applications. It was shown that Nafion® can be premixed with cationic proteins, such as cytochrome *c*, and that these mixtures produce, at the air-electrolyte interface, interfacial layer which can be compressed and transferred on solid substrates in a typical LB experiment [162]. The deposition of these ultrathin films on electrodes gives modified electrodes useful for (bio)electrocatalysis and biosensing purposes.

Because of the polymeric nature of the ionomers, the LB films obtained are characterized by a certain 2-D packing and ordering (more relevant for the perfluorinated ionomers), however, they do not achieve a complete spreading of the ion-exchange sites on a 2-D "monomolecular" sheet, but tend to achieve a sort of flattened-entangled structure [161]. Further studies are required to better understand the real (supra)molecular structure of these films as well as the dependence of the surface properties of the coated electrodes on the number of deposition steps or chemical nature of incorporated redox counterions.

Anyway, the Langmuir-Blodgett technique looks like a new attractive way to control the deposition of ionomers even for relatively large scale preparation of stocks of modified electrodes obtained under strictly controlled conditions.

2.5.3. Coating Regeneration

When considering the analytical applications of ion-exchange voltammetry, it is important to assess the regenerability (reusability) of the modified surface. If the ion-exchange selectivity coefficient for the analyte is not too large, regeneration can be achieved by simply exposing the film to a high concentration of nonelectroactive salt solution so obtaining expulsion of the analyte from the ion-exchanger film. However, such a simple regeneration procedure cannot be successful for analytes characterized by very large ion-exchange selectivity coefficients. For this reason, a number of studies were devoted to two alternative approaches which can overcome this problem; they are:

- prepare single use electrodes based on the preparation of cheap and disposable electrode systems such as screen-printed electrodes [163, 164];
- developing coatings which can facilitate the regeneration of the ion-exchange membranes.

The modifiers used for the preparation of screen-printed electrodes are typically different from the polymeric membrane systems which are the subject of the present chapter, so we will not go into many details of this approach.

The regenerability of the coatings can be improved by developing polymer films whose net charge can be switched chemically and/or electrochemically from positive to neutral to negative. Pioneering studies in this direction were carried out in Anson's group where poly(4-vinylpyridine) [165] and poly(2-vinylpyrazine) [41], containing electroactive pendant groups such as $[Fe(CN)_5^{3-/2-}]$, were used to this aim. In the case of electrodes coated with poly(4-vinylpyridine), three types of charged groups, namely protonated pyridinium cations (pH switchable), pentacyanoferrate anions (potential switchable) and quaternized pyridinium cations (unswitchable) were introduced in the same polymeric coating [165]. Hence, by changing both the applied potential and the solution pH, it was possible to change the net charge from 0.4+ to 0.4− per pyridine group, thus allowing the preconcentration and complete release of electroactive cations or, alternatively, anions.

A similar approach, in which the ion-exchange characteristics were modulated only by electrochemical switching, implied ter-polymers based on styrene (backbone), styrenesulfonate (unswitchable cation-exchanger) and vinyl-ferrocene (electrochemically switchable from neutral to anion-exchanger) [166, 167]. When the Fc/Fc$^+$ couple in the film was reduced, the terpolymer acted as a cation-exchanger. When Fc was oxidized, the electrogenerated Fc$^+$ cation became the counter-ion for the SO_3^- groups, thus allowing the release of the incorporated cations (analyte). The switching from cation-exchanger to neutral polymer was achieved also by using electrodes coated with conducting polymer and polyelectrolytes composites [168, 177]. Typical examples of such an approach were the electrochemically controlled binding and release of cations at poly(N-methyl-pyrrole)/poly(styrene-sulfonate) [175] or at polypyrrole/poly(ester-sulphonate)[177]. When the conducting polymer was reduced, cations such as protonated amines, $Ru(bpy)_3^{2+}$ or methylviologen were incorporated into the film, while the release of these compounds was accomplished by simple reoxidation [165].
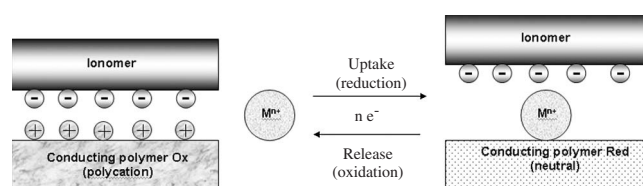
Figure 3. Schematic representation of the uptake-release of the redox cation M^{n+} at electrochemically switchable ionomer/conducting polymers composites.

More recently these principles were applied for developing solid phase microextraction (SPME)electrodes in which the redox switching of the conducting polymer was exploited for performing the electrochemically controlled uptake and release of ionic analytes [178–181].

General principles of functioning of electrochemically switchable ion-exchanger/conducting polymer composites are summarized in Fig. 3.

By taking advantage of the anion preconcentration capabilities of oxidized conducting polymers, Mark and co-workers [178] used a Pt microfiber coated with poly(3-methylthiophene) (PMeT) to perform the electrochemically controlled extraction and desorption of arseniate anions. The extension of this principle to cationic analytes was presented recently by Nyholm and co-workers [181], who used polypyrrole films doped with anions of low mobility in order to obtain a film which in the reduced states acts as cation exchanger.

All these studies were performed using aqueous solution as the sample. However, both from a SPME viewpoint and when thinking to chromatographic applications of electrochemically switchable ion-exchange devices [182], the development of electrochemically switchable polymer films usable in organic solvents is rather attractive; recently, a composite between poly(3-methylthiophene) and poly-estersulphonate was developed to this aim [183]. Note that, among the ionomers used as coatings on electrode surfaces, AQ55® is the only one which is both stable and which shows very good cation exchange properties also in acetonitrile solutions [83, 126, 184].

The development of ionomer based SPME devices can open the way to extended application of IEV for environmental electroanalysis and in electrochemically controllable separation methods.

3. POLYMERS AS TEMPLATE FOR NANOELECTRODE ENSEMBLES

3.1. Template Synthesis of Nanoelectrode Ensembles

Nanoelectrode ensembles (NEEs) and arrays (NEAs) are new electroanalytical tools which can find application in a variety of fields ranging from sensors to electronics, from energy storage to magnetic materials [15]. The difference between NEEs and NEAs is that in the former the spatial distribution of the nanoelectrodes is random while in the array it is ordered. In the following we will refer generically to NEEs with the majority of the considerations being easily transferable to NEAs. As already presented in the
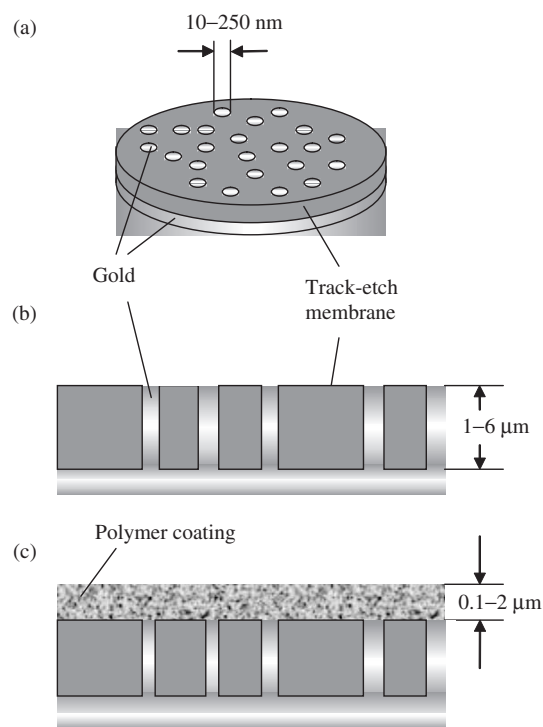
general introduction, NEEs can be prepared using microporous membranes as templating systems. In the template synthesis of NEEs developed by Martin et al. [11], a metal (generally gold) is electroless deposited into the pores of nanoporous membranes. The scheme of the structure of a NEE is shown in Fig. 4.

Historically, the template synthesis was introduced by Possin [185] and refined by Williams and Giordano [186] who prepared different metallic wires with diameter as small as 10 nm within the pores of etched nuclear damage tracks in mica. Electrochemical deposition of nanowires of metals (e.g., Ni and Co) [187], of semiconductors [188], oxides [189] and conducting polymers [15] was performed.

Other approaches are based on exploiting as NEEs the defects generated in self assembled monolayers [190–192]. Nanoelectrodes have been fabricated also creating and controlling the pores in a block copolymer self assembled matrix [193] as well as by exploiting chemical self-assembly of colloids [194].

Arrays of nanoelectrodes have been prepared very recently also by using optical fiber bundles coated with gold [195, 196] or by indium tin oxide [199]. The chemical etching of the fiber bundle's distal end results in arrays of tips which are coated with the metal; individual nanotips can be obtained by coating the base of the fiber array with electrophoretic paint. Such devices present an interesting combination of optical and electrochemical properties.

At the present status of research, in all these arrays and ensembles all the nanoelectrodes are connected each other by a back metal current collector so that all experience the same applied potential during voltammetric experiments.

In the template synthesis of nanoelectrode ensembles, each pore of a microporous membrane is filled with a metal nanowire or nanofiber. The metal fiber growth can be performed both using electrochemical [8, 187] or electroless deposition [11] methods. For the former case, one side of the membrane must be made conductive, for instance, by sputtering a thin layer of gold, while for the latter a chemical sensitization of the membrane is required [11]. With both deposition methods, the diameter of the pores in the template determines the diameter of the Au-disk nanoelectrode elements that make up the NEE. Membranes with pore diameters ranging from 10 μm to 10 nm can be obtained commercially. The density of the pores in the template determines the number of Au-disk nanoelectrode elements per cm^2 of NEE surface and, correspondingly, the average distance between the nanoelectrode elements.

There are two classes of microporous membranes which can be used as template for NEEs fabrication: alumina membranes and track-etched polymeric membranes, both shown for comparison in Fig. 5.

The alumina membranes are prepared by controlled anodization of aluminum [200, 201]; they are also commercially available. As a consequence of their preparation method, they are characterized by very high pore densities so that the ratio between the pores area/overall geometric area is a number not much smaller than unity [see
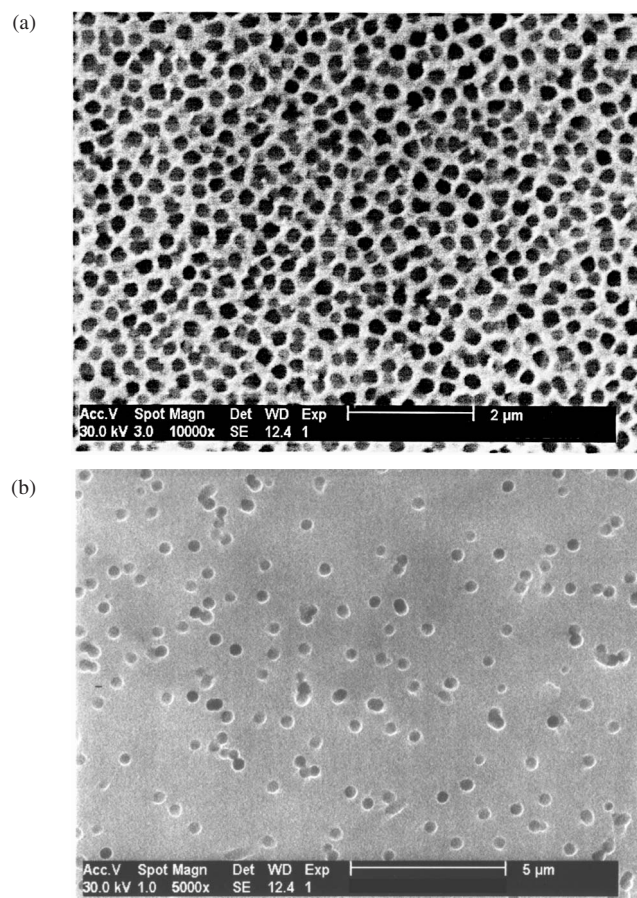
Figure 4. Scheme of a nanoelectrode ensemble in a template membrane: (a) overall view; (b) lateral section; (c) lateral section of a polymer coated nanoelectrode ensemble.

Figure 5. SEM images of commercial microporous membrane with pores of 200 nm diameter: (a) alumina; (b) track-etched polycarbonate.

Fig. 5(a)]. As explained in the following paragraph, for taking advantage of the electrochemical peculiarities of NEEs it is important to start the template synthesis from membranes characterized by much smaller pore densities. For this reason the alumina membranes are scarcely used as templates for NEEs fabrication, while they are widely and successfully used for the fabrication of a variety of other template based nanostructures and nanodevices [202].

As shown in Fig. 5(b), track-etched polymeric membranes are indeed characterized by much smaller pore densities. There are two methods of producing latent tracks in polymer foils to be transformed in porous membranes. One is based on the irradiation of the polymer foil with nuclear fission fragments of heavy elements such as californium or uranium. The second is based on the use of ion beams from accelerators. Both methods have their advantages and peculiarities [203]. The tracking of the polymer foil is then followed by chemical etching, that is the pore formation process. The tracked zone is removed by the chemical etching agent, typically a solution of a strong alkali. The chemical etching determines the pore size and shape [203–205], while the time of tracking determines the pore density [203, 207]. Polymeric materials most widely used for preparing track-etched porous membranes are polycarbonate, polyethylene terephthalate and polyimide [203].

Commercially available track-etch membranes contains monodisperse cylindrical pores, with diameter from 10 nm to few micrometers and pore densities in the 10^6–10^8 pores/cm^2 range; the surface of a typical NEE prepared by electroless deposition of Au nanofibers in a polycarbonate membrane (pores diameter 30 nm) is shown in Fig. 6. However, some laboratories are using specially-made membranes, with geometric characteristics slightly different from the commercial ones [206, 207].

3.2. Electrochemical Properties of Nanoelectrode Ensembles

3.2.1. Diffusion at NEE

The characteristics that distinguish NEEs and NEAs from conventional macro (mm-sized) or even ultramicro
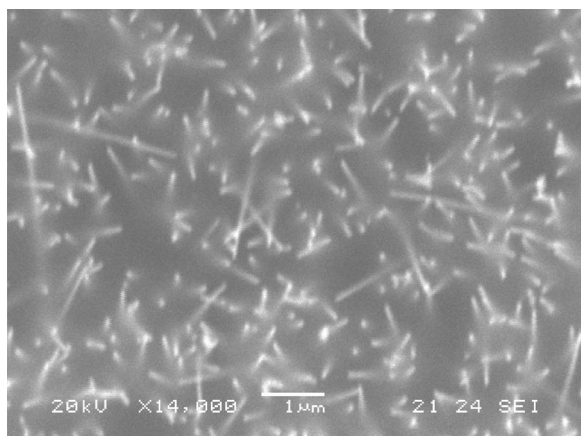
Figure 6. SEM image of a NEE prepared by electroless deposition of gold fibers within the pores (30 nm diameter) of a commercial track-etched polycarbonate membrane.

(μm-sized) electrodes are:

- dramatic lowering of double layer charging (capacitive) currents [11, 12];
- extreme sensitivity to the kinetics of the charge transfer process [208], which means capability to measure very high charge transfer rate constants [190].

Since these characteristics are peculiar to nanoelectrode ensembles, in case of experimental inability to get direct morphological information on the NEE structure by e.g., electron or scanning probe microscopy [209], the lack of some of these characteristics, such as the persistence of high capacitive currents, should be taken as a diagnostic indication of a failure in the preparation procedure.
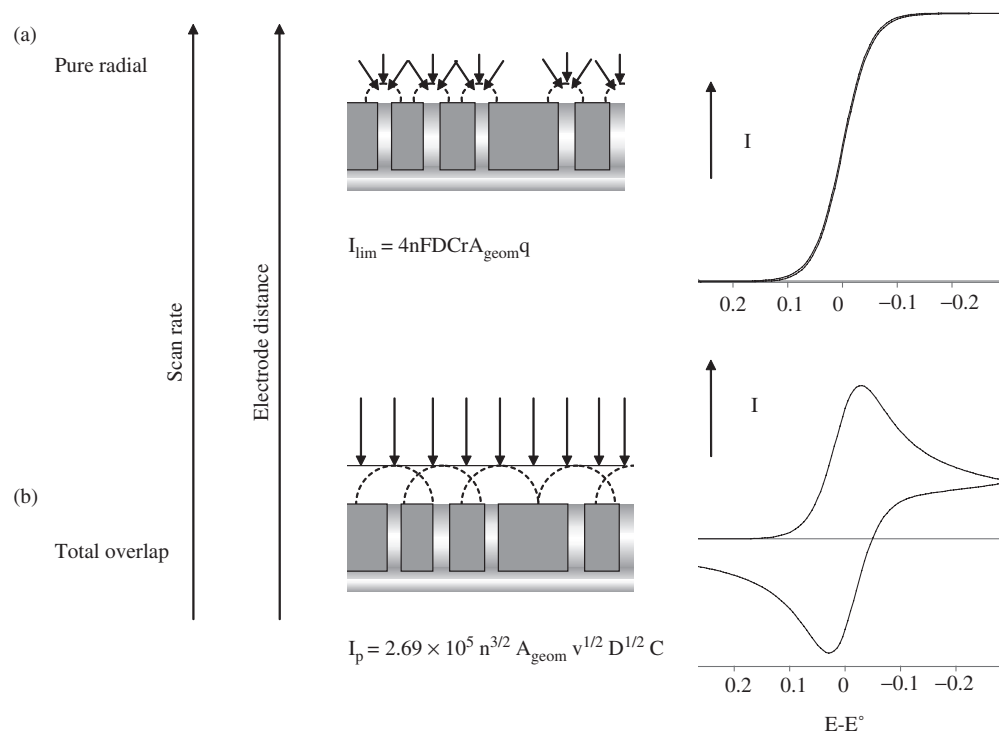
From a voltammetric viewpoint, NEE can be considered as ensembles of disc ultramicroelectrodes separated by an electrical insulator interposed between them. An ultramicroelectrode is considered as an electrode with at least one dimension comparable or lower than then the thickness of the diffusion layer (typically <25 μm). At such small electrodes, edge effects from the electrode become relevant and diffusion from the bulk solution to the electrode surface is described in terms of radial geometry instead of the simpler linear geometry used for larger (>100 μm) electrodes. Under radial diffusion control, the voltammogram displays a typical sigmoidal shape; a limiting current (I_{lim}) instead of a peak, is the relevant analytical parameter related diredctly to the analyte concentration.

A NEE can be considered as a very large assembly of very small ultramicrolectrodes confined in a rather small space. The density (q) of nanodiscs/surface in a NEE is large (10^6–10^8 elements/cm^2); for this reason, all the nanoelectrodes are statistically equivalent and the different contribution of the elements at the outer range of the ensemble can be considered negligible [210, 211] even in NEEs of overall area as small as 10^{-2}–10^{-3} cm^2 [210].

NEEs can exhibit three distinct voltammetric response regimes depending on the scan rate or reciprocal distance between the nanoelectrode elements [206, 212]. When radial diffusion boundary layers overlap totally (radius of diffusion hemisphere larger then average hemidistance between electrodes, slow scan rates) NEEs behave as planar macroelectrodes with respect to Faradaic currents (total overlap conditions). When diffusion hemispheres become shorter (higher scan rates), the current response is dominated by radial diffusion at each single element(pure radial conditions). At very high scan rates, the linear active state is reached in which the current response is governed by linear diffusion to the individual nanodisc. Figure 7 sketches the situation encountered for the total overlap and pure radial regimes; being characterized by the higher signal/background current ratios (see below), these two regimes are those typically used for analytical and sensing applications.

The diffusion regime usually observed at NEEs prepared from commercial track-etched membranes is the total overlap regime [11]. Transition from one regime to the other as a function of nanoelements distance was demonstrated experimentally [206] using specially-made membranes.

$I_{lim} = 4nFDCrA_{geom}q$

(a) Pure radial

(b) Total overlap

Scan rate

Electrode distance

I

I

0.2   0.1   0   −0.1   −0.2

$I_p = 2.69 \times 10^5\ n^{3/2}\ A_{geom}\ v^{1/2}\ D^{1/2}\ C$

0.2   0.1   0   −0.1   −0.2

E-E°

Figure 7. Typical diffusive regimes observed at nanoelectrode ensembles as a function of the scan rate and/or nanoelectrodes distance. See text for symbols in the equations.

3.2.2. Signal to Background Current Ratios

Under total overlap diffusion regime, NEEs show enhanced electroanalytical detection limits, relative to a conventional millimeter-sized electrode. This is because the Faradaic current (I_F) at the NEE is proportional to the total geometric area (A_{geom}, nanodiscs plus insulator area) of the ensemble, while the double-layer charging current (I_C) is proportional only to the area of the electrode elements (active area, A_{act}) [11]; in voltammetry, I_C is the main component of the background.

Faradaic-to-capacitive currents at NEEs and conventional electrodes with the same geometric area are related by Eq. (18) [6, 11]:

$$(I_F/I_C)_{NEE} = (I_F/I_C)_{conv}\ A_{geom}/A_{act} \tag{18}$$

This ratio at the NEE is higher than the relevant ratio at a conventional electrode of the same geometric area for a proportionality factor that is the reciprocal of the fractional electrode area f, defined as

$$f = A_{act}/A_{geom} \tag{19}$$

Typical f values for NEEs are between 10^{-3} and 10^{-2}. Such an improvement in the Faradaic to capacitive currents ratio explains why detection limits (DLs) at NEEs can be 2–3 order of magnitude lower than with conventional electrodes [11, 12, 213].

It was shown that improvements in signal/background current ratios at NEEs are independent on the total geometric area of the ensemble [210]; this is true if the fractional area is kept constant and if the dimensions of the ensemble are lowered to a size still large enough to contain a large number of nanoelements (for instance, NEE with A_{geom} of 0.005 cm² contains 4.8×10^6 nanoelectrodes). Note that NEEs warranty such an independence on the ensemble size for overall geometric areas much lower than those required for achieving comparable results with arrays of micrometer sized electrodes [211]. This is particularly attractive when thinking to apply the advantages of the use of arrays/ensembles of micro-nanoelectrodes to analyses in samples of very small volume or for "*in vivo*" biomedical applications.

For a given overall geometric area, it is evident that the I_F/I_C is maximum when the total overlap regime is operative, being lower in the case of a pure radial regime. In this case, in fact, only a certain percentage of the geometric area of the ensemble contribute to producing a Faradaic current while, in the total overlap regime, this percentage is 100%. On the other hand, it is worth stressing that for NEEs or NEAs with the same active area, higher Faradaic currents are achieved when operating under pure radial conditions [211]; this is the regime of choice for obtaining the maximum improvement of detection limits when there is no constrain in increasing the distance between the nanoelectrode elements and/or the overall geometric area of the ensemble.

It was shown that NEEs can be used not only as naked nanoelectrode ensembles, but also as polymer coated devices [see Fig. 4(c)] [12]. For instance, the overall surface of a NEE (insulator and nanodiscs) can be easily coated by a thin layer of an ionomer coating. In the cited literature example [12], the ionomer of choice was the

polyestersulphonate Eastman AQ55®, which was applied as a water dispersion, i.e., using a solvent which does not damage the NEE surface (the polycarbonate template can be damaged by organic solvents). Really, such an approach showed that it was possible to combine successfully the preconcentration capabilities of ionomer coated electrodes with the increased Faradaic/capacitive current ratio typical of NEEs. From a detection limit viewpoint, it was advantageous to use polymer-coated NEEs operating under total overlap conditions and not under radial diffusion control, in order to keep as low as possible the negative effect of the decrease of (apparent) diffusion coefficients related to the ion-exchange incorporation of the redox analyte. As said before, in the total overlap regime, responses obey the Randles-Sevcik equation with peak currents depending on $D^{1/2}$ and not directly on D, as it is the case for the pure radial diffusive regime [60].

The ability of NEEs to furnish well resolved cyclic voltammograms for trace redox species has interesting consequences also for adsorption related problems, as in the case of small organic redox molecules and some biomacromolecules as well. If adsorption is concentration dependent, then lowering the solution concentration below the adsorption limit can sometime overcome the problem. This was demonstrated to be the case for some phenothiazines [213], commonly used as redox mediators in biosensors, and for the heme-containing enzyme cytochrome *c* [214].

3.2.3. Electron Transfer Kinetics

An important characteristics of NEEs is that electron transfer kinetics appear slower than at single electrodes [11]. Being composed of a large number of nanodiscs metal elements surrounded by a large surface of insulating material (the guest membrane), NEEs can be considered as electrodes with partially blocked surface (PBE); the nanodiscs electrodes are the unblocked surface and the template membrane is the blocking material. According to the pioneering model elaborated by Amatore et al. [208], the current response at this kind of electrodes is identical to that at a naked electrode of the same overall geometric area, but with a smaller apparent standard rate constant for the electron transfer which decreases as the coverage with the blocking agent increases. Such an apparent rate constant (k°_{app}) is related, in fact, to the true standard charge transfer rate constant (k°), by the relationship [208]:

$$k^\circ_{app} = k^\circ(1 - \vartheta) = k^\circ f \qquad (20)$$

where ϑ is the fraction of blocked electrode surface and f is the fraction of the electrode surface that is Au nanodisks [see Eq. (19)].

Such a dependence has two different practical consequences. From a mechanistic viewpoint, it is an advantage since it means that with NEEs it is easier to obtain experimentally very large k° values [19]. What is measured at NEE is indeed the smaller k°_{app}, which can be converted into the larger k° by means of Eq. (20) [190, 213].

From an analytical viewpoint, the operativity of Eq. (19) means that, at NEEs, high Faradaic current signals are obtained only for redox systems who behaves "very" reversibly [11]. In cyclic voltammetry, the reversibility

depends on k° and the scan rate; at a regular electrode a redox system gives a reversible voltammetric pattern when $k^\circ > 0.3$ $v^{1/2}$ cm s^{-1} [19]. At NEEs k_{app} substitutes k°; this means that at a NEE a redox system gives a reversible

Table 4. Examples of analytical applications of nanoelectrode ensembles.

Analyte	Comments	Ref.
Ferrocene derivatives, $Ru(NH_3)_6^{3+}$	Fundamentals for the fabrication and characterization of Au-NEEs are given. It is shown that DL can be 3 orders of magnitude lower than with regular electrodes.	[11]
Ferrocene derivatives, $Ru(NH_3)_6^{3+}$	NEE coated with polyestersulphonate are used for preconcentration and trace analyses of redox cations. DL are in the 10^{-9} M range.	[12]
$Fe(CN)_6^{4-}$	NEE fabricated by self-assembly of Au colloidal nanoparticles. Electrode density depends on self-assembly time. DL = 1×10^{-8} M.	[194]
Phenotiazine, methylviologen	Cathodic limit at Au-NEE is examined. Detection limits depend on reduction potential: DL = 1.2×10^{-7} M for phenothiazine, 2×10^{-6} M for methylviologen.	[213]
Cytochrome *c*	Au-NEE detect the direct electrochemistry of cyt *c* even in the absence of promoters. Dilute solutions avoid adsorption problems. DL = 1×10^{-6} M by CV and 3×10^{-8} M by DPV.	[210, 214]
NO	Pt-NEE in an alumina template is designed for NO determination *in vitro* and *in vivo*. Interfering anions are rejected by a Nafion® coating. DL = 1×10^{-8} M	[217]
Glucose	Au nanotubular electrode ensemble used for in flow detection of glucose. Glucose oxidase immobilized via bonding to self assembled monolayers deposited on Au. DL = 2×10^{-4} M	[218]
Glucose	Carbon nanotube (CNT)-NEE is fabricated. Glucose oxidase immobilized on CNT via carbodiimide. H_2O_2 detected catalytically by CNT. DL = 8×10^{-5} M	[219]
DNA duplex	Interdigited array of 100 nm electrodes fabricated by e-beam lithography. DNA is attached to Au and $Ru(NH_3)_6^{3+}$ is used as redox intercalator. Characterization of *ss*- and *ds*-DNA of 15 nucleotides performed	[220]
DNA duplex	NEA of multiwalled CNT embedded in SiO_2. DNA attached to CNT via carbodiimide. Detection by $Ru(bpy)_3^{2+}$ mediated guanine oxidation.	[221]
DNA duplex	3-D NEEs are obtained by partial etching with oxygen plasma from 2-D NEEs in polycarbonate template. Detection of duplex formation at attomole-level is achieved by Ru(III)/Fe(III) electrocatalysis.	[222]

voltammetric pattern when $k° > k_{app}/f$, i.e., $k° > 3 \times 10^2$ v$^{1/2}$ cm s^{-1} when, for instance, f is 10^{-3} [6]. With fixed pore density, the excessive lowering of the nanodiscs diameter can increase the irreversibility problem. This is a limitation to be seriously taken into account when trying to optimize NEEs for analytical application, since it is important to consider the contrasting effect both of the increased I_F/I_C value and the apparent slowing down of the electron transfer kinetics. On the other hand, it is worth pointing out that the high sensitivity of NEEs to electron transfer kinetics can be even turned into an advantage, to avoid the effect of interfering substances when the interences are sluggish redox couples while the analyte is an electrochemically (very) reversible redox species.

Further understanding of the electrochemical behavior of NEEs will probably take advantage of recent studies devoted to modeling by digital simulation the voltammetric behavior of regular [215] and random arrays [216] of ultramicroelectrodes.

3.2.4. Analytical and Sensing Applications of NEE

The ability of NEEs to furnish well resolved cyclic voltammograms allowed researchers to develop sensitive methods for trace determinations of redox species characterized by fast electron transfer kinetics. For this reason, the analytes of choice for such applications are mainly redox molecules displaying very reversible voltammetric behavior as those typically employed as electron transfer mediators in biosensors. Note that lowering the background interference (double-layer charging current) in an electrochemical determination improves not only the detection limit, but also the precision of the determination.

Table 4 lists some analytical application of NEEs. It is evident that, up to now, NEEs applications are oriented mainly toward the development of advanced electrochemical biosensors. It is worth to note that the analytical applications of NEE are just at their beginning and that such electrode systems, for their peculiarities, are expected to contribute significantly to the growth of more sensitive and extremely miniaturized electrochemical sensors.

4. CONCLUSIONS AND PROSPECTS

The use of polymeric materials both attached to coat electrode surfaces or used as template to built nanostructured ensembles of microscopic electrodes, has contributed significantly to develop a new class of tailored electrochemical sensors characterized by very high sensitivity and very low detection limit, both characteristics being improved dramatically with respect to conventional electrodes.

Ion-exchange voltammetry at ionomer coated electrodes has grown progressively up to reaching nowadays the rank of a widespread powerful electroanalytical technique. It is suitable for trace and ultratrace analyses and can be used as a valuable tool in speciation analysis for environmental studies and biomedicine. The ionomer coating gives to the electrode high sensitivity and selectivity and protects it from surfactants and organics interferences. Further efforts should be devoted in the near future to continue improving the reproducibility and control of the coating deposition procedure

and to shorten the analysis time. The application of molecular engineering procedures such as LB, electrostatic spray, layer by layer deposition can play a crucial role in this issue.

Nanoelectrode ensembles show dramatically enhanced signal to background current ratios with respect to any other electrode system, however with the limitation of giving the maximum in these performances for reversible redox systems. Such a limit can be turned into an advantage if NEEs will be used in electrochemical biosensors where electron transfer processes are tuned by the electrochemistry of suitable reversible mediators. The combination of ion-exchange voltammetry and NEEs appears as a powerful tool to push voltammetric techniques toward simpler, faster, more sensitive and selective detection schemes.

Future research efforts need to be devoted for evolving from the present NEEs (where all nanoelectrodes are connected each other) to more sophisticated arrays of singly addressable (groups of) nanoelectrodes. The call for advanced analytical devices able to cope with multiple analytes determinations in samples of very small volume, is asking for the extreme miniaturization of chemical sensing devices, included electrochemical ones. Such requirements are peculiar for sensors to be used in the bioanalytical field, both for "*in vitro*" and "*in vivo*" analyses, however, the advantages coming from the availability of multianalytes sensors are obvious also for environmental or food analyses and for materials testing as well.

Because of their small dimensions, the very favorable signal/background current ratio and the possibility to link receptor molecules directly on their surface, nanoelectrode ensembles and polymeric coatings are expected to play a key role in the future development of advanced electrochemical sensors.

GLOSSARY

Analyte Element, ion or molecule whose presence and concentration is being detected in a sample by suitable analytical procedures.

Amphiphile Molecule composed by two parts: one that by itself would mix with water (hydrophilic) and another that by itself would not (hydrophobic). Amphilies are also named surfactants.

Biosensor Self contained device which provides specific analytical information using a biological recognition element in direct contact with a transduction element. For the case of an electrochemical biosensor, the transduction element is an electrode.

Diffusion Spontaneous mass transport movement of molecules or ions under the influence of a concentration gradient. Its driving force is the tendency to minimize concentration differences in the sample. The flux of diffusing molecules is proportional to the diffusion coefficient (a constant characteristic of the molecule under study and the solution medium) and the concentration gradient.

Double layer Array of charged particles (ions) and/or oriented dipoles present at the interface between a charged surface and a solution. In an electrochemical experiment, the charging of the electrode surface causes the built up of the double layer which reflects in the generation of a capacitive current (a non-faradaic current).

Electrochemistry   Branch of chemistry concerned with the interrelation between electricity and chemistry. It studies chemical changes caused by the passage of an electric current and the production of electrical energy by chemical reactions. Electrochemistry is involved in a variety of phenomena from corrosion to energy storage and production, from electrolytic and galvanic processes to electrochemical methods of analysis.

Electrochemical sensor   Sensing device which employs electrochemical transducers (electrodes) interconnected with chemical recognition layers to transform specific chemical information (presence and /or concentration of one or a group of specific components of the sample) into an analytically useful signal.

Electrode   Electronic conductor (metal) in contact with a ionic conductor (electrolyte), connected to a suitable electrical apparatus able to provide/measure electric potential and/or electric current.

Faradaic process   Electron transfer reaction in which charges (electrons) are transferred at the electrode-solution interface to cause the oxidation or reduction of a chemical substance. Faraday's law states that the amount of chemical reaction caused by the flow of current is proportional to the amount of electricity passed.

Ionomer   Ionic polymer characterized by a small content of ionic groups. Typically, block copolymers made of alternate linear arrangements of blocks of ionic and blocks of un-polar monomers.

Ion-exchange   Reversible interchange of ions between a solid and a liquid in which there is no permanent change in the structure of the solid. The solid is named ion-exchanger.

Langmuir-Blodgett films   Ordered molecular layers obtained from monolayers of amphiphilic molecules. They are formed by controlled 2-D compression in the LB trough of a monomolecular layer of amphiphilic molecules spread at the air/water interface. The 2-D ordered interfacial layer can be transferred onto solid surfaces by controlled dipping of the substrate through the interface.

Layer-by-layer   Chemical procedure which allows the construction of sandwiched layers of ionic molecules of opposite charge, assembled by exploiting favorable electrostatic interactions.

Limit of detection   The lowest concentration of an analyte which gives a signal distinguishable from the background noise. It is usually calculated as the ratio between three-times the standard deviation of the background signal and the analytical sensitivity.

Potentiometry   Static (zero current) electroanalytical technique in which the information on the sample composition is obtained from the measurement of the difference in potential established across two sides of a membrane or between a suitable indicator electrode and a reference electrode.

Speciation analysis   Analytical activity aimed to identifying and/or measuring the quantities of one or more individual chemical species of an element in a sample.

Track-etch   Procedure for obtaining nano- or micro-porous membranes from thin sheets of materials such as mica or some organic polymers. Latent tracks are produced by irradiation with fission fragments of heavy nuclei in a nuclear reactor or by ion beams from accelerators. During chemical etching, usually with alkali solutions, the damaged zones are removed and transformed in hollow channels (pores).

Transducer   Device which converts a form of energy into another one. Transducers used in chemical instrumentation generate an electronic signal (e.g., a voltage) proportional to a chemical or physical property of the analyte; for instance, a photomultiplier in a spectrophotometer produces an electric current proportional to the number of photons.

Sensitivity   The ratio between the change in analytical signal caused by a change in the concentration of the analyte. If the signal and concentration are related by a linear relationship, it is given by the slope of the linear calibration plot.

Voltammetry   Dynamic electroanalytical technique in which the information on the sample composition is obtained from a current signal generated by a time-dependent electric potential stimulation applied to an electrochemical cell. The electrochemical cell is made by three electrodes (working, reference and auxiliary, or counter, electrode) dipped in the sample solution. Voltammetry can measure any chemical species which is electroactive, i.e., which can be oxidized or reduced at the electrode-solution interface.

ACKNOWLEDGMENTS

REFERENCES

1. N. Oyama and F. C. Anson, *J. Electrochem. Soc.* 127, 247 (1980).
2. I. Rubinstein and A. J. Bard, *J. Am. Chem. Soc.* 102, 6641 (1980).
3. R. W. Murray, *Philos. Trans. R. Soc. London, Ser. A* 302, 253 (1981)
4. R. W. Murray, in "Electroanalytical Chemistry" (A. J. Bard, Ed.), Vol. 13, p. 155. Marcel Dekker, New York, 1984.
5. P. Ugo and L. M. Moretto, *Electroanalysis* 7, 1105 (1995).
6. (a) P. Ugo, L. M. Moretto, and F. Vezzà, *Chem. Phys. Chem.* 3, 917 (2002); (b) P. Ugo, L. M. Moretto, and F. Vezzà, in "Sensors Update" (H. Baltes, G. K. Fedder, and J. G. Korvink, Eds.), Vol. 12, p. 121. Wiley-VCH, Weinheim, 2003.
7. J. M. Zen, A. S. Kumar, D. M. Tsai, *Electroanalysis* 15, 1073 (2003).
8. R. M. Penner and C. R. Martin, *Anal. Chem.* 59, 2625 (1987).
9. I. F. Cheng and C. R. Martin, *Anal. Chem.* 60, 2163 (1988).
10. K. Uosaki, K. Okazaki, H. Kita, and H. Takahashi, *Anal. Chem.* 62, 652 (1990).
11. V. P. Menon and C. R. Martin, *Anal. Chem.* 67, 1920 (1995).
12. P. Ugo, L. M. Moretto, S. Bellomi, V. P. Menon, and C. R. Martin, *Anal. Chem.* 68, 4160 (1996).
13. A. Ulman, "Ultrathin Organic Films." Academic Press, San Diego, 1991.
14. G. Decher, *Science* 277, 1232 (1997).
15. C. R. Martin in "Electroanalytical Chemistry" (A. J. Bard and I. Rubinstein, Eds.), Vol. 21, p. 1. Marcel Dekker, New York, 1999.
16. H. H. Thorp, C. R. Loomis, and M. E. Napier, US Patent 5,968,745, 1999.
17. T. G. Drummond, M. G. Hill, and J. K. Barton, *Nat. Biotechnol.* 21, 1192 (2003).

18. K. Dill, D. D. Montgomery, A. L. Ghindilis, and K. R. Schwarzkopf, *J. Biochem. Biophys. Methods* 59, 181 (2004).
19. A. J. Bard and L. Faulkner, "Electrochemical Methods," 2nd Edition. Wiley, New York, 2000.
20. J. Wang, "Analytical Electrochemistry," 2nd Edition. VCH, Weinheim, 2000.
21. N. Fatouros, J. P. Simonin, J. Chevalet, and R. M. Reeves, *J. Electroanal. Chem.* 213, 1 (1986).
22. D. Krulic, N. Fatouros, and J. Chevalet, *J. Electroanal. Chem.* 287, 215 (1990).
23. L. M. Moretto, P. Ugo, R. Lacasse, G. Y. Champagne, and J. Chevalet, *J. Electroanal. Chem.* 467, 193 (1999).
24. L. M. Moretto, J. Chevalet, G. A. Mazzocchin, and P. Ugo, *J. Electroanal. Chem.* 498, 117 (2001).
25. Kh. Brainina and E. Neyman, "Electroanalytical Stripping Methods in Chemical Analysis." John Wiley, New York, 1993.
26. J. Wang, in "Electroanalytical Chemistry" (A. J. Bard, Ed.), Vol. 16, p. 1. Marcel Dekker, New York, 1989.
27. J. Buffle, "Complexation Reactions in Aquatic Systems—An Analytical Approach." Ellis Horwood, Chichester, 1988.
28. M. Wojciechouski, W. Go, and J. Osteryoung, *Anal. Chem.* 57, 155 (1985).
29. C. Colombo and C. van den Berg, *Anal. Chim. Acta* 337, 229 (1998).
30. Ø. Mikkelsen and K. H. Schroeder, *Anal. Lett.* 33, 3253 (2000).
31. J. Wang, J. Lu, U. A. Kirgoz, S. B. Hocevar, and D. Ogorevc, *Anal. Chim. Acta* 434, 29 (2001).
32. R. Murray, in "Molecular Design of Electrode Surfaces" (R. Murray, Ed.), p. 1. John Wiley, New York, 1992.
33. F. Helfferich, "Ion Exchange." McGraw-Hill, New York, 1962.
34. M. W. Espencheid, A. R. Ghatak-Roy, R. B. Moore III, R. M. Penner, M. N. Szentirmay, and C. R. Martin, *J. Chem. Soc. Faraday Trans. I* 82, 1051 (1986).
35. B. Hoyer, T. M. Florence, and G. E. Batley, *Anal. Chem.* 1987, 59, 1608–1614.
36. B. Hoyer and T. M. Florence, *Anal. Chem.* 59, 2839–2842.
37. C. M. A. Brett, D. A. Fungaro, J. M. Morgado, and M. H. Gil, *J. Electroanal. Chem.* 468, 26(1999).
38. C. M. A. Brett and D. A. Fungaro, *Talanta* 50, 1223 (2000).
39. R. Naegeli, J. Redepenning, and F. C. Anson, *J. Phys. Chem.* 90, 6227 (1986).
40. J. Redepenning and F. C. Anson, *J. Phys. Chem.* 91, 4549 (1987).
41. P. Ugo and F. C. Anson, *Anal. Chem.* 61, 1799 (1989).
42. R. Toniolo, N. Comisso, G. Bontempelli, and G. Schiavon, *Talanta* 41, 473 (1994).
43. P. Ugo, L. M. Moretto, A. De Boni, P. Scopece, and G. A. Mazzocchin, *Anal. Chim. Acta* 474, 147 (2002).
44. A. R. Hillman, in "Electrochemical Science and Technology of Polymers" (R. G. Linford, Ed.), Vol. 1, p. 103. Elsevier Applied Science, London, 1987.
45. M. Majda, in "Molecular Design of Electrode Surfaces" (R. Murray, Ed.), p. 159. John Wiley, New York, 1992.
46. N. Oyama, in "Molecular Design of Electrode Surfaces" (R. Murray, Ed.), p. 333. John Wiley, New York, 1992.
47. M. N. Szentirmay and C. R. Martin, *Anal. Chem.* 56, 1898 (1984).
48. P. Ugo, B. Ballarin, S. Daniele, and G. A. Mazzocchin, *J. Electroanal. Chem.* 324, 145 (1992).
49. F. B. Kaufman and E. M. Engler, *J. Am. Chem. Soc.* 101, 547 (1979).
50. J. Facci and R. W. Murray, *J. Phys. Chem.* 85, 2870 (1981).
51. D. A. Buttry and F. C. Anson, *J. Am. Chem. Soc.* 105, 685 (1983).
52. F. C. Anson, D. N. Blauch, J. M. Saveant, and C. F. Shu, *J. Am. Chem. Soc.* 113, 1922 (1991).
53. H. I. Dahms, *J. Phys. Chem.* 72, 362 (1968)
54. I. Ruff and V. J. Friedrich, *J. Phys. Chem.* 75, 3297 (1971).
55. L. D. Whiteley and C. R. Martin, *J. Phys. Chem.* 93, 4650 (1989).
56. K.-N. Kuo and R. W. Murray, *J. Electroanal. Chem.* 131, 37 (1982).
57. M. Majda and L. R. Faulkner, *J. Electroanal.Chem.* 169, 77 (1984).
58. C. R. Martin, I. Rubinstein, and A. J. Bard, *J. Am. Chem. Soc.* 104, 4817 (1982).
59. M. Shi and F. C. Anson, *Anal. Chem.* 69, 2653 (1997).
60. S. Daniele, P. Ugo, C. Bragato, and G. A. Mazzocchin, *J. Electroanal. Chem.* 418, 29 (1996).
61. C. Amatore, C. Sella, and L. Thouin, *J. Electroanal. Chem.* 547, 151 (2003).
62. J. I. Kroschwitz, "Concise Encyclopedia of Polymer Science and Engineering," pp. 495. J. Wiley, New York, 1990.
63. R. S. Yeo and H. L. Yeager, "Modern Aspects of Electrochemistry" (B. E. Conway, R. E. White, and J. O'M. Bockris, Eds.), Vol. 16, p. 437. Plenum Press, New York, 1985.
64. L. A. Zook, *J. Leddy, Anal. Chem.* 68, 3793 (1996).
65. T.-Y. Chen and J. Leddy, *Langmuir* 16 2866 (2000).
66. K. J. Oberbroeckling, D. C. Dunwoody, S. D. Minteer, and J. Leddy, *Anal. Chem.* 74, 4794 (2002).
67. F. C. Anson, J. M. Saveant, and K. Shigehara, *J. Am. Chem. Soc.* 105, 1096 (1983).
68. A. Walcarius, *Electroanalysis* 13, 701 (2001).
69. J.-M. Zen and Y.-S. Ting, *Anal. Chim. Acta* 332, 59 (1996).
70. J. C. Vidal, G. Cepria, and J. R. Castillo, *Anal. Chim. Acta* 259, 129 (1992).
71. Z. Hu, C. J. Seliskar, and W. R. Heineman *Anal. Chim. Acta* 369, 93 (1998).
72. R. R. Dalangin and H. Gunasingham, *Anal. Chim. Acta* 291, 81 (1994).
73. J. C. Vidal, R. B. Vinao, and J. R. Castillo, *Electroanalysis* 4, 653 (1992).
74. R.D. Guy, and S. Namaratne, *Can. J. Chem.* 65, 1133 (1987).
75. T.-H. Lu, H.-Y. Yang, and I.-W. Sun, *Talanta* 49, 59 (1999).
76. R. Toniolo, G. Bontempelli, G. Schiavon, and G. Zotti, *J. Electroanal. Chem.* 356, 67 (1993)
77. P. Ugo, L. M. Moretto, D. Rudello, E. Birriel, and J. Chevalet, *Electroanalysis* 13, 661 (2001).
78. P. Ugo, F. Cavalieri, D. Rudello, L. M. Moretto, and E. Argese, *Sensors* 1, 102 (2001).
79. L. M. Moretto, B. Brunetti, J. Chevalet, and P. Ugo, *Electrochem. Commun.* 2, 175 (2000).
80. P. Ugo, B. Ballarin, S. Daniele, and G. A. Mazzocchin, *J. Electroanal. Chem.* 291, 187 (1990).
81. P. Ugo, B. Ballarin, S. Daniele, and G. A. Mazzocchin, *Anal. Chim. Acta* 244, 29 (1991).
82. J. Wang, Z. Lu, *J. Electroanal. Chem.* 266, 287 (1989).
83. B. Brunetti and P. Ugo, *J. Electroanal. Chem.* 460, 38 (1999).
84. T.-H. Lu and I.-W Sun, *Talanta* 53, 443 (2000).
85. B. Barroso-Fernandez, M. T. Lee-Alvarez, C. J. Seliskar, and W. R. Heineman, *Anal. Chim. Acta* 370, 221 (1998).
86. J. M. Zen, S. H. Jeng, and H. J. Chen, *Anal. Chem.* 68, 498 (1996).
87. S. D. Collyer, S. E. Bradbury, J. V. Hatfiled, and S. P. J. Higson, *Electroanalysis* 13, 332 (2001).
88. J.-M. Zen, J.-J. Jou, and A. S. Kumar, *Anal. Chim. Acta* 396, 39 (199).
89. H. Yi, K. Wu, S.Hu, and D. Cui, *Talanta* 55, 1205 (2001).
90. J. Wang, and P. Tuzhi, *Anal. Chem.* 58, 3257 (1986).
91. J. Wang, P. Tuzhi, and T. Golden, *Anal. Chim. Acta* 194, 129 (1987).
92. J. Wang and T. Golden, *Anal. Chem.* 61, 1397 (1989).
93. M. P. Brazell, R. J. Kasser, K. J. Renner, J. Feng, B. Moghaddam, and R. N. Adams, *J. Neurosci. Methods* 22, 167 (1987).
94. E. W. Kristensen and R. M. Wightman, *Anal. Chem.* 59, 1752 (1987)
95. F. Crespi, K. F. Martin, and C. A. Marsden, *Neuroscience* 27, 885 (1988).
96. O. Niwa, M. Morita, and H. Tabei, *Electroanalysis* 6, 237 (1994).
97. J. Litong, L. Shonghui, B. Zhuping, and F. Yuzhi, *Electroanalysis* 5, 611 (1993).
98. W. Gorski and J. A. Cox, *Anal. Chem.* 64, 2706 (1992).

99. J. Zhou, and E. Wang, *Anal. Chim. Acta* 249, 489 (1991).

100. D. Boyd, J. R. Barreira Rodriguez, A. J. Miranda Ordieres, P. Tunon Blanco, and M. R. Smyth, *Analyst* 119, 1979 (1994).

101. B. D. Coleman, *Electroanaalysis* 16, 1393 (2004).

102. H.-L. Cheng and I.-W. Sun, *Electroanalysis* 13, 1544 (2001).

103. W. Surareungchai and D. Kasiwat, *Electroanaalysis* 12, 1124 (2000).

104. J. A. Cox and P. J. Kulesza, *Anal. Chim. Acta* 154, 71 (1983).

105. J. A. Cox and P. J. Kulesza, *J. Electroanal. Chem.* 159, 337 (1983).

106. G. Schiavon, G. Zotti, R. Toniolo, and G. Bontempelli, *Anal. Chim. Acta* 264, 221 (1992).

107. P. Ugo, L. M. Moretto, and G. A. Mazzocchin, *Anal. Chim. Acta* 305, 74 (1995).

108. L. M. Moretto, G. A. Mazzocchin, and P. Ugo, *J. Electroanal. Chem.* 427, 113 (1997).

109. P. Ugo, L. Sperni, and L. M. Moretto, *Electroanalysis* 9, 1153 (1997).

110. P. Ugo, L. Sperni, and G. A. Mazzocchin, *Ann. Chim. (Rome)* 92, 301 (2002).

111. J.-M. Zen and M.-J. Chung, *Anal. Chim. Acta* 320, 43 (1996).

112. T.-H. Lu, H.-Y.-Yang, and I.-W. Sun, *Talanta* 49, 59 (1999).

113. T.-H. Lu and I.-W. Sun, *Electroanalysis* 10, 1052 (1998).

114. T.-H. Lu, J.-F. Huang, and I.-W. Sun, *Anal. Chim. Acta* 454, 93 (2001).

115. J.-M. Zen, H.-G. Chung, and G. Ilagovan, *Electroanalysis* 11, 108 (1999).

116. J. F. Cassidy, and K. Tokuda, *J. Electroanal. Chem.* 59, 740 (1987).

117. P. Ugo., L. M. Moretto, and G. A. Mazzocchin, *Anal. Chim. Acta* 273, 229 (1993).

118. H.-Y. Yang, and I.-W. Sun, *Anal. Chem.* 72, 3476 (2000).

119. J. Wang and T. Golden, *P. Tuzhi, Anal. Chem.* 59, 740 (1987).

120. H. Mao and P. G. Pickup, *J. Electroanal. Chem.* 265, 127 (1989).

121. H.-L. Cheng, C.-H. Kuei, and I. W. Sun, *Electroanalysis* 14, 767 (2002).

122. D. A. Buttry and F. C. Anson, *J. Electroanal. Chem.* 130, 333 (1981).

123. L. Dunsch, L. Kavan, and J. Weber, *J. Electroanal. Chem.* 280, 313 (1990).

124. F. B. Kaufman, A. H. Schroeder, E. M. Engler, S. R. Kramer, and J. Q. Chambers, *J. Am. Chem. Soc.* 102, 483 (1980).

125. A. H. Schroeder and F. B. Kaufman, *J. Electroanal. Chem.* 113, 209 (1980).

126. T. Gennett and W. C. Purdy, *Anal. Chem.* 62, 2155 (1990).

127. J. Weber, P. Janda, L. Kavan, and A. Jegorov, *J. Electroanal. Chem.* 200, 379 (1986).

128. R. B. Moore III and C. R. Martin, *Macromolecules* 21, 1334 (1988).

129. G. Goebel, P. Aldebert, and M. Pineri, *Macromolecules* 20, 1425 (1987).

130. B. Hoyer and N. Jensen, *Talanta* 41, 449 (1994).

131. K. A. Stribel, G. G. Scherer, and O. Haas, *J. Electroanal. Chem.* 304, 289 (1991).

132. M. Shi and F. C. Anson, *J. Electroanal. Chem.* 415, 41 (1996).

133. K. Shimazu, H. Kita, and T. Kuwana, *J. Electroanal. Chem.* 258, 49 (1989).

134. H. Nishide, J. Deguchi, and E. Tsuchida, *J. Polymer Sci.* 15, 3023 (1977).

135. B. Lindholm and M. Sharp, *J. Electroanal. Chem.* 198, 37 (1986).

136. N. Oyama, T. Shimomura, K. Shigehara, and F. C. Anson, *J. Electroanal. Chem.* 112, 271 (1980).

137. E. S. De Castro, E. W. Huber, D. Villaroel, C. Galiatsatos, J. E. Mark, W. R. Heineman, and P. T. Murray, *Anal. Chem.* 59, 134 (1987).

138. P. Denisevich, H. D. Abruna, C. R. Leidner, T. J. Meyer, and R. W. Murray, *Inorg. Chem.* 21, 2152 (1982).

139. R. B. Kaner, in "Electrochemical Science and Technology of Polymers" (R. G. Linford, Ed.), Vol. 2, p. 97. Elsevier, London, 1990.

140. P. G. Pickup, *J. Electroanal. Chem.* 225, 273 (1987).

141. S. Basak and K. Rajeshwar, *M. Kaneko, Anal. Chem.* 62, 1407 (1990).

142. S. Cosnier, A. Deronzier, J.-C. Moutet, and J. F. Roland, *J. Electroanal. Chem.* 271, 69 (1989).

143. A. R. Guadalupe and H. D. Abruna, *Anal. Chem.* 57, 142 (1985).

144.

145.

146. B. Hoyer, N. Jensen, and L. P. Busch, *Electroanalysis* 13, 843 (2001).

147. I. Wilner, and E. Katz, *Angew. Chem., Int. Ed.* 39, 1180 (2000).

148. N. Mano, and A. Kuhn, *Bioelectrochemistry* 56, 123 (2002).

149. N. Mano Kuhn, *Biosens. Bioelectron.* 16, 653 (2001).

150. N. Anicet, C. Bourdillon, J. Moiroux, and J.-M. Saveant, *J. Phys. Chem. B* 102, 9845 (1998).

151. J. Hodak, R. Etchenique, E. J. Calvo, K. Singhal, and P. N. Bartlett, *Langmuir* 13, 2708 (1997).

152. H. Ma, N. Hu, and J. Rusling, *Langmuir* 16, 4969 (2000).

153. E. Lojou and P. Bianco, *J. Electroanal. Chem.* 557, 37 (2003).

154. E. Lojou and P. Bianco, *Langmuir* 20, 748 (2004).

155. I. Galeska, D. Chattopadhyay, F. Moussy, and F. Papadimitrakopoulos, *Biomacromolecules* 1, 2002 (2000).

156. J. J. Harris, J. L. Stair, and M. Bruening, *Chem. Mater.* 12, 1941 (2000).

157. E. J. Calvo and A. Wolosiuk, *J. Am. Chem. Soc.* 124, 8490 (2002).

158. D. M. DeLongchamp and P. T. Hammond, *Chem. Mater.* 15, 1165 (2003).

159. P. Bertoncello, M. K. Ram, A. Notargiacomo, P. Ugo, and C. Nicolini, *Phys. Chem. Chem. Phys.* 4, 4036 (2002).

160. P. Bertoncello and P. Ugo, *J. Braz. Chem. Soc.* 14, 517 (2003).

161. P.Ugo, P. Bertoncello, and F. Vezzà, *Electrochim. Acta* 49, 3785 (2004).

162. L. M. Moretto, P. Bertoncello, F. Vezzà, and P. Ugo, *Bioelectrochemistry* In press.

163. S. A. Wring and J. P. Hart, *Analyst* 117, 1281 (1992).

164. P. Ugo, L. M. Moretto, P. Bertoncello, and J. Wang, *Electroanalysis* 10, 1017 (1998).

165. H. R. Zumbrunnen and F. C. Anson, *J. Electroanal. Chem.* 152, 111 (1983).

166. M. W. Espenscheid and C. R. Martin, *J. Electroanal. Chem.* 188, 73 (1985).

167. M. W. Espenscheid and C. R. Martin, *Electroanalysis* 1, 93 (1989).

168. F. F. Fan and A. J. Bard, *J. Electrochem. Soc.* 133, 301 (1986).

169. R. M. Penner and C. R. Martin, *J. Electrochem. Soc.* 133, 310 (1986).

170. G. Nagasubramanian, S. Di Stefano, and J. Moacanin, *J. Phys. Chem.* 90, 4447 (1986).

171. D. Orata and D. A. Buttry, *J. Electroanal. Chem.* 257, 71 (1988).

172. T. Hirai, S. Kuwabata, and H. Yonegani, *J. Electrochem. Soc.* 135, 1132 (1988).

173. T. Shimidzu, A. Ohtani, T.Iyoda, and K. Honda, *J. Electroanal. Chem.* 224, 123 (1987).

174. T. Shimidzu, A. Ohtani, T.Iyoda, and K. Honda, *J. Electroanal. Chem.* 251, 323 (1988).

175. Q. X. Zhou, L. L. Miller, and J. R. Valentine, *J. Electroanal. Chem.* 261, 147 (1989).

176. C. M. Elliot, A. B. Kopelove, W. J. Albery, and Z. Chen, *J. Phys. Chem.* 95, 1743 (1991).

177. J. Wang, Z. Sun, and Z. Lu, *J. Electroanal. Chem.* 310, 269 (1991).

178. T. P. Gbatu, O. Ceylan, K. L. Sutton, J. F. Rubinson, A. Galal, J. A. Caruso, and H. B. Mark, *Anal. Commun.* 36, 203 (1999)

179. J. Wu, X. Yu, H. Lord, and J. Pawliszyn, *Analyst* 125, 391 (2000).

180. J. Wu and J. Pawliszyn, *J. Chromatogr.* 909, 37 (2001).

181. G. Liljegren, J. Petterson, K. E. Markides, and L. Nyholm, *Analyst* 127, 591 (2002).

182. R. S. Deinhammer, M. D. Porter, and K. Shimazu, *J. Electroanal. Chem.* 387, 35 (1995).

183. P. Scopece, L. M. Moretto, and P. Ugo, *J. Electroanal. Chem.* submitted.
184. J. Hanzlik, P. Ugo, S. Daniele, and G. A. Mazzocchin, *J. Electroanal. Chem.* 404, 89(1996).
185. G. E. Possin, *Rev. Sci. Instrum.* 41, 772 (1970).
186. W. D. Williams, and N. Giordano, *Rev. Sci. Instrum.* 55, 410 (1984).
187. C. Schoennberger, B. M. I. van der Zande, L. G. J. Fokkink, M. Henny, C. Schmid, M. Kruger, A. Bachtold, R. Huber, H. Birk, and U. Staufer, *J. Phys. Chem. B* 101, 5497 (1997).
188. D. Routkevitch, T. Bigioni, M. Moskovits, and J.-M. Xu, *J. Phys. Chem.* 100, 14037 (1996).
189. M. Zheng, G. Li, X. Zhang, S. Huang, Y. Lei, and L. Zhang, *Chem. Mater.* 13, 3859 (2001).
190. E. Sabatani and J. Rubinstein, *J. Phys. Chem.* 91, 6663 (1987).
191. O. Chailapakul, L. Sun, C. J. Xu, and R. M. Crooks, *J. Am. Chem. Soc.* 115, 12459 (1993).
192. G. L. Che and C. R. Cabrera, *J. Electroanal. Chem.* 417, 155 (1996).
193. E. Jeonng, T. H. Galow, J. Schotter, M. Bal, A. Ursache, M. T. Tuominen, C. M. Stafford, T. P. Russel, and V. M. Rotello, *Langmuir* 17, 6396 (2001).
194. W. Cheng, S. Dong, and E. Wang, *Anal. Chem.* 74, 3599 (2002).
195. P. Pantano, and D. R. Walt, *Rev. Sci. Instrum.* 68, 1357 (1997).
196. J. M. Tam, S. Szunerits, and D. R. Walt, in "Enciclopedia of Nanoscience and Technology" (H. S. Naiwa, Ed.). American Scientific Publishers, Stevenson Ranch, 2003.
197. S. Szunerits, P. Garrigue, J.-L. Bruneel, L. Servant, and N. Sojic, *Electroanalysis* 15, 548 (2003).
198. S. Szunerits, J. M. Tam, L. Thouin, C. Amatore, and D. R. Walt, *Anal. Chem.* 75 4382 (2003).
199. A. Chovin, P. Garrigue, P. Vinatier, and N. Sojic, *Anal. Chem.* 76, 357 (2004).
200. J. W. Diggle, T. C. Downie, and C. W. Goulding, *Chem. Rev.* 69, 365 (1969).
201. A. Despic and V. P. Parkhutik, in "Modern Aspects of Electrochemistry" (J. O'M. Bockris, R. E. White, and B. E. Conway, Eds.), Vol. 20, p. 401. Plenum Press, New York, 1989.
202. J. C. Hulteen and C. R. Martin, *J. Mater. Chem.* 7, 1075 (1997).
203. P. Apel, *Radiat. Meas.* 34, 559 (2001).
204. Z. Siwy and A. Fulinski, *Phys. Rev. Lett.* 89, 198, 103 (2002).
205. Z. Siwy, D. Dobrev, R. Neumann, C. Trautmann, and K. Voss, *Appl. Phys. A* 76, 781 (2003).
206. J. C. Hulteen, V. P. Menon, and C. R. Martin, *J. Chem. Soc. Faraday Trans.* 92, 4029 (1996).
207. N. Li, S. Yun, C. C. Harrell, and C. R. Martin, *Anal. Chem.* 76, 2025 (2004).
208. C. Amatore, J. M. Saveant, and D. Tessier, *J. Electroanal. Chem.* 147, 39 (1983).
209. W. S. Baker and R. M. Crooks, *J. Phys. Chem. B* 102, 10041 (1998).
210. L. M. Moretto, N. Pepe, and P. Ugo, *Talanta* 62, 1055 (2004).
211. H. J. Lee, C. Beriet, R. Ferrigno, and H. H. Girault, *J. Electroanal. Chem.* 502, 138 (2001)
212. J. F. Cheng, L. D. Whiteley, and C. R. Martin, *Anal. Chem.* 61, 762 (1989).
213. B. Brunetti, P. Ugo, L. M. Moretto, and C. R. Martin, *J. Electroanal. Chem.* 491, 166(2000).
214. P. Ugo, N. Pepe, L. M. Moretto, and M. Battagliarin, *J. Electroanal. Chem.* 560, 51 (2003).
215. B. A. Brookes, T. J. Davies, A. C. Fisher, R. G. Evans, S. J. Wilkins, K. Yunus, J. D. Wadhawan, and R. G. Compton, *J. Phys. Chem. B* 107, 1616 (2003).
216. T. J. Davies B. A. Brookes, A. C. Fisher, K. Yunus, S. J. Wilkins, P. R. Green, J. D. Wadhawan, and R. G. Compton, *J. Phys. Chem. B* 107, 6431 (2003).
217. Y. Xian, M. Liu, Q. Cai, H. Li, J. Lu, and L. Jin, *Analyst* 126, 871 (2001)
218. M. Delvaux, S. Demoustier-Champagne, and A. Walcarius, *Electroanalysis* 16, 190 (2004).
219. Y. Lin, F. Lu, Y. Tu, and Z. Ren, *Nano Lett.* 4, 191 (2004).
220. E. Finot, E. Bourillot, R. Meunier-Prest, Y. Lacroute, G. Legay, M. Cherkaoui-Malki, N. Latruffe, O. Siri, P. Braunstein, and A. Dereux, *Ultramicroscopy* 97, 441 (2003).
221. J. Li, H. T. Ng, A. Cassell, W. Fan, H. Chen, Q. Ye, J. Koehne, J. Han, and M. Meyyappan, *Nano Lett.* 3, 597 (2003).
222. R. Gasparac, B. J. Taft, M. A. Lapierre-Devlin, A. D. Lazareck, J. M. Xu, and S. O. Kelly, *J. Am. Chem. Soc.* 126, 12270 (2004).